High sensitive luminescent ratiometric thermometer based on europium(III) and terbium(III) benzoylacetonate complexes chemically bonded to ethyldiphenylphosphine oxide functionalized polydimethylsiloxane

D.A. Gálico, I.O. Mazali, F.A. Sigoli*

Laboratory of Functional Materials – Institute of Chemistry - University of Campinas – UNICAMP

Campinas, Sao Paulo, Brazil, P.O. Box 6154, 13083-970

Email: fsigoli@iqm.unicamp.br

Supporting Information

Figures:

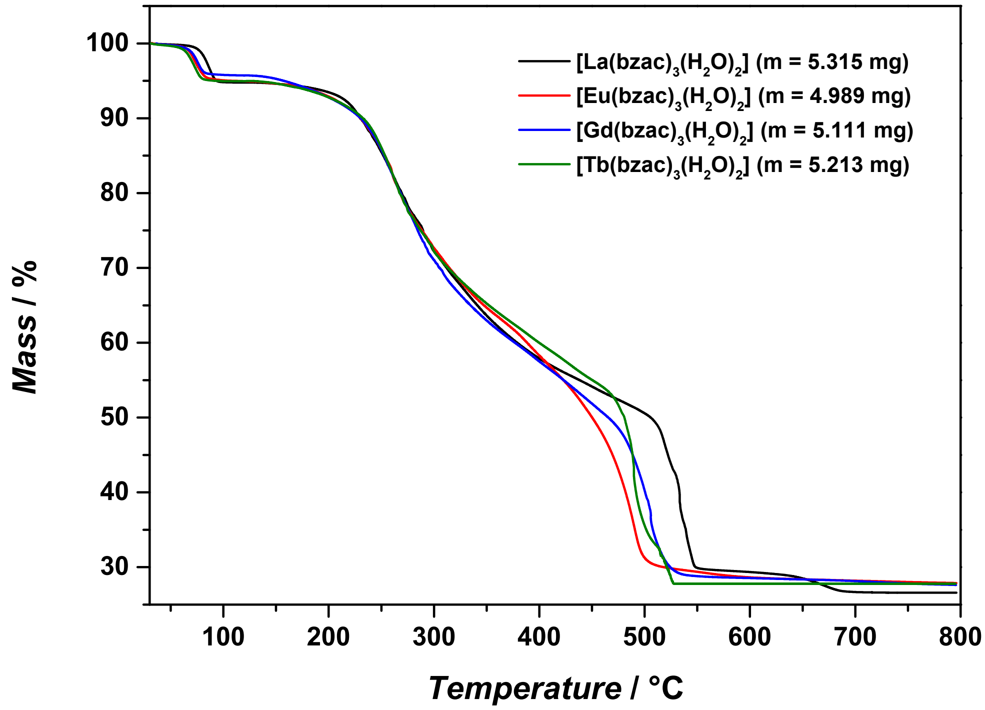

Figure S1: Thermogravimetric curves of the complexes.

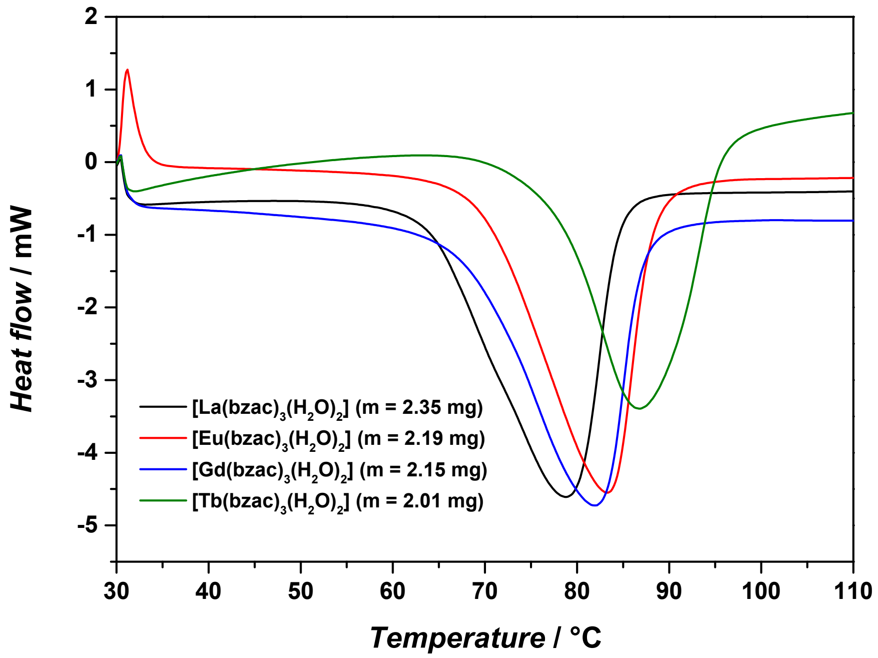

Figure S2: DSC curves of the complexes.

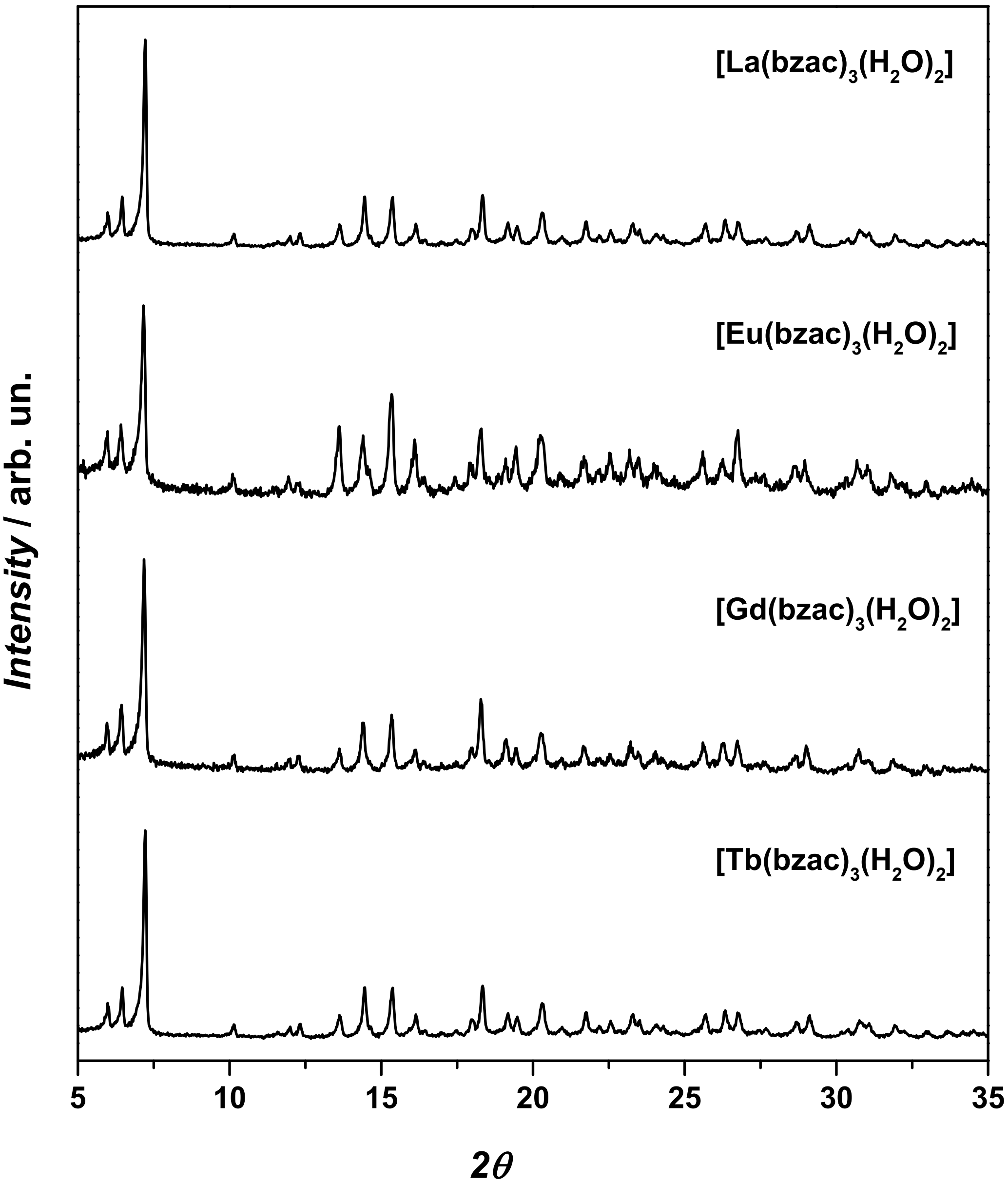

Figure S3: X-Ray diffraction patterns of the complexes.

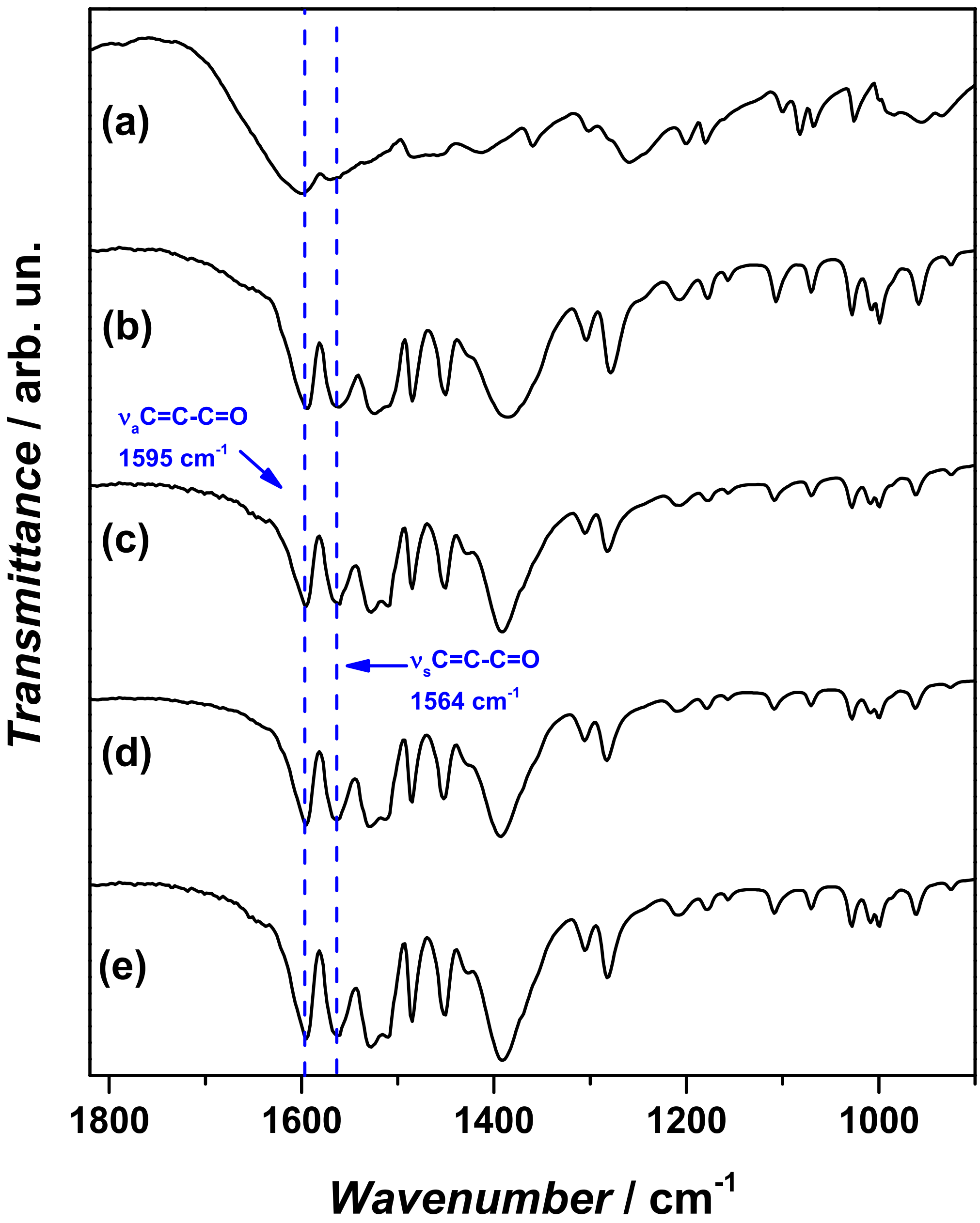

Figure S4: FTIR spectra of (a) benzoylacetone ligand, (b) [La(bzac)$_3$(H$_2$O)$_2$], (c) [Gd(bzac)$_3$(H$_2$O)$_2$], (d) [Tb(bzac)$_3$(H$_2$O)$_2$] and (e) [Eu(bzac)$_3$(H$_2$O)$_2$].

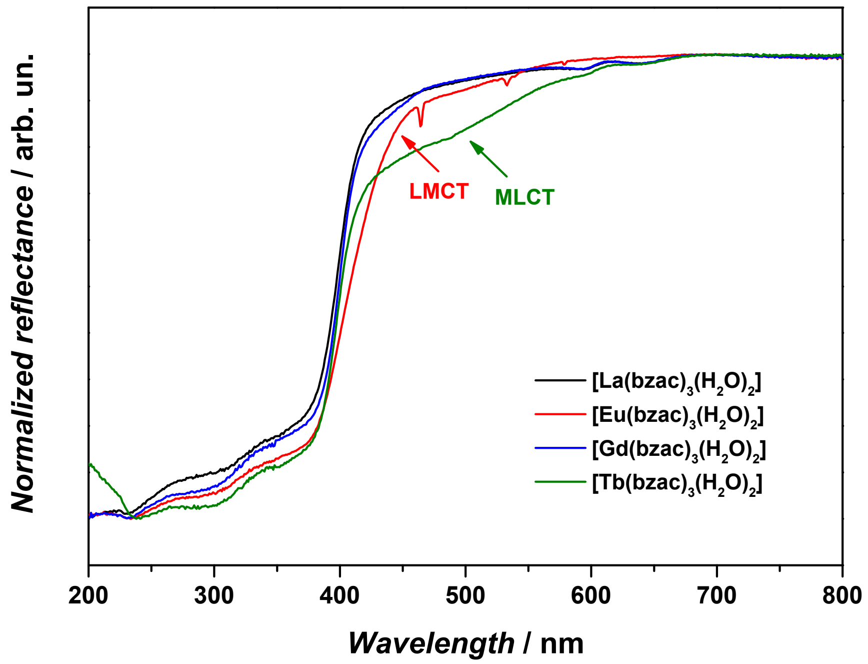

Figure S5: Diffuse reflectance spectra of the complexes.

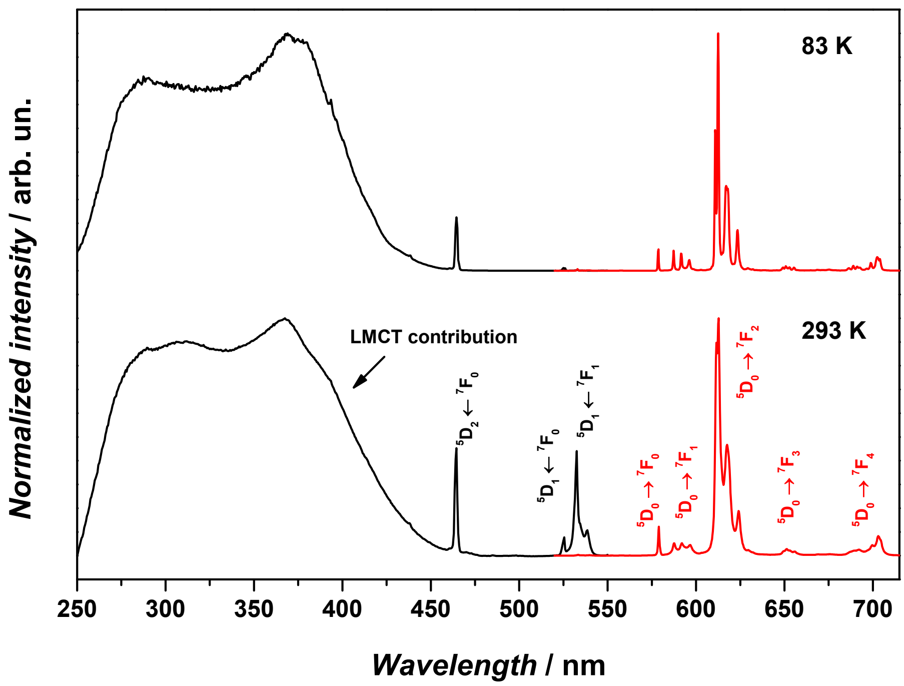

Figure S6: Excitation (black line, λ_{em} = 612 nm) and emission (red line, λ_{ex} = 360 nm) of the $[Eu(bzac)_3(H_2O)_2]$ complex at 83 and 293 K.

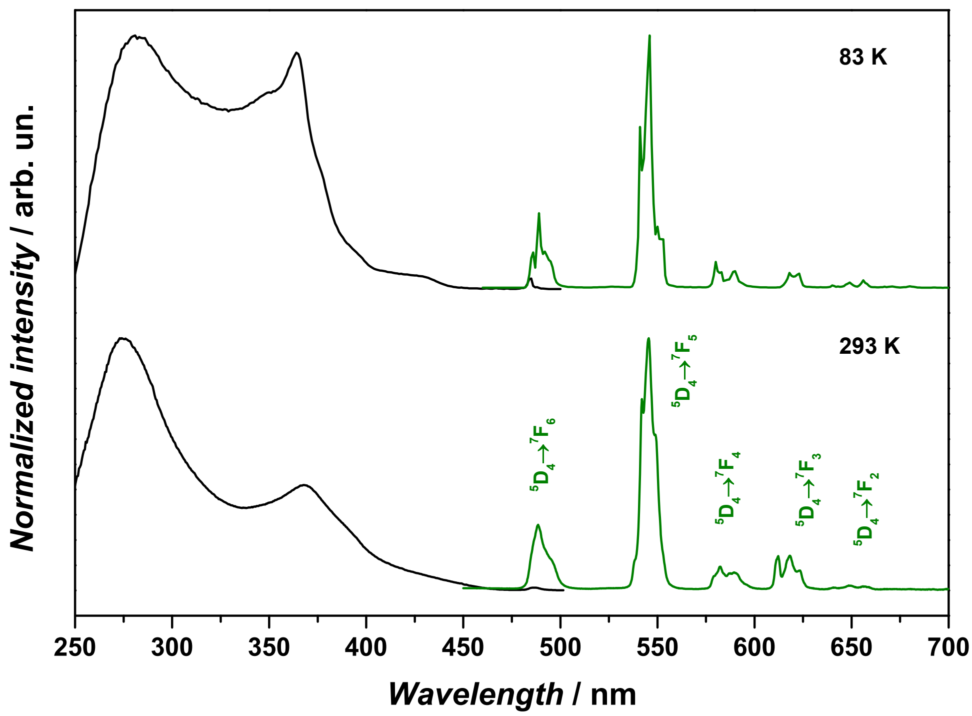

Figure S7: Excitation (black line, λ_{em} = 546 nm) and emission (red line, λ_{ex} = 360 nm) of the $[Tb(bzac)_3(H_2O)_2]$ complex at 83 and 293 K.

.

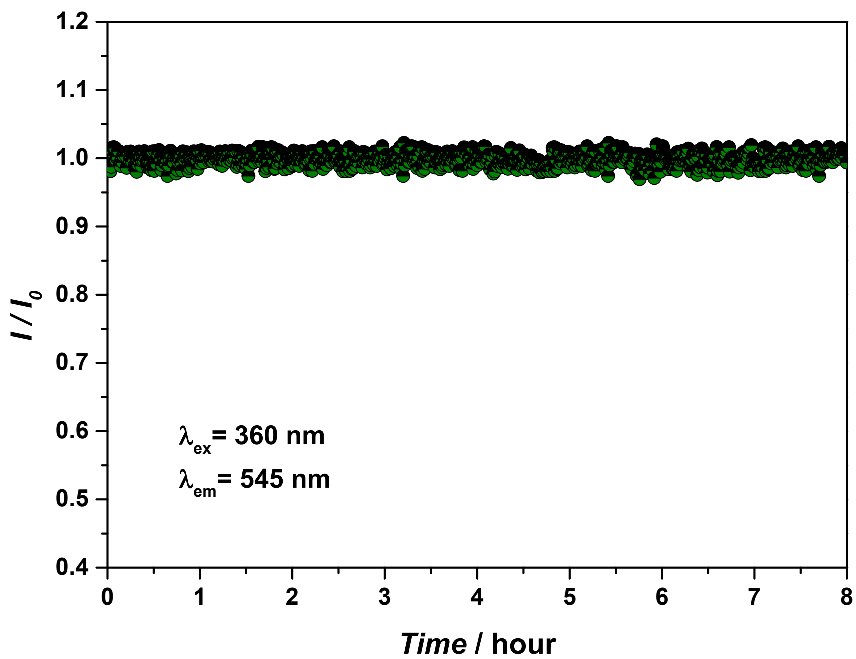

Figure S8: Photostability study of the $[Tb(bzac)_3(H_2O)_2]$ in air atmosphere.

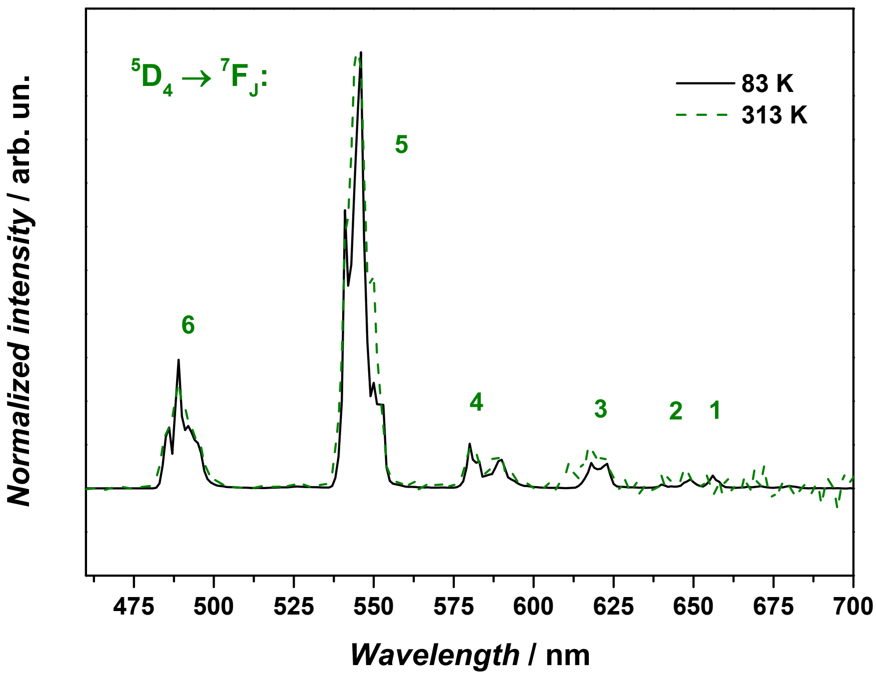

Figure S9: Comparison between 83 and 313 K emission spectra of $[Tb(bzac)_3(H_2O)_2]$ complex.

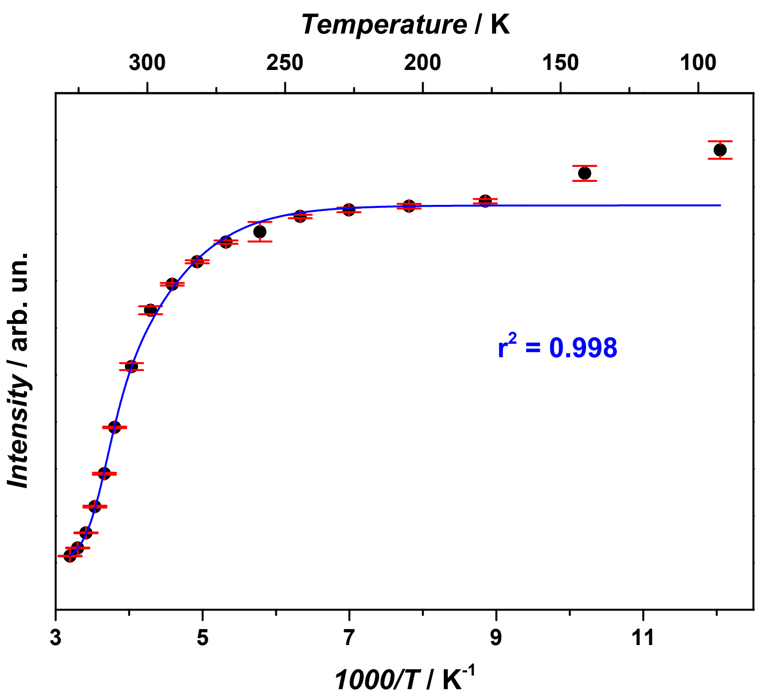

Figure S10: Temperature dependence of the integrated area of the emission spectra of $[Tb(bzac)_3(H_2O)_2]$. The solid line represents the data of the best fit (r^2=0.998) of the Mott-Seitz model involving two non-radiative recombination channels.

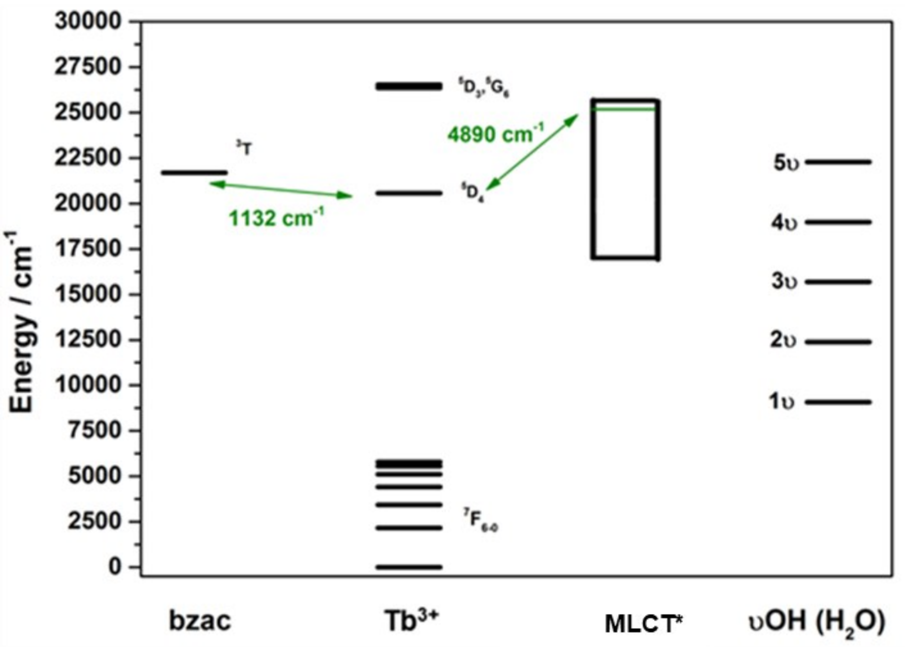

Figure S11: Partial energy diagram of [Tb(bzac)$_3$(H$_2$O)$_2$] complex. *As described in the manuscript, the assignment of this energy level is out of the scope of this work and here we consider that this band may be attributed to a MLCT state, although this assumption is controversial in the literature.

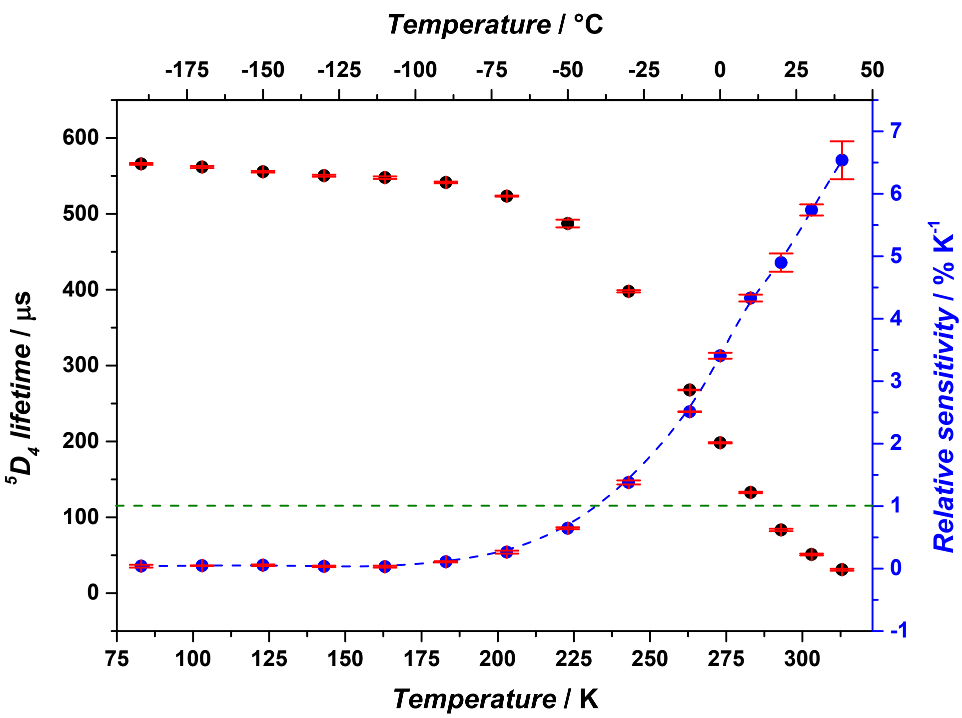

Figure S12: Temperature dependence of $^5D_4$ emitter state lifetime and the obtained relative sensitivity of the [Tb(bzac)$_3$(H$_2$O)$_2$] complex (λ_{ex} = 360 nm / λ_{em} = 545 nm); green line is only a guide for the eyes indicating the relative sensitivity of 1 % K^{-1}.

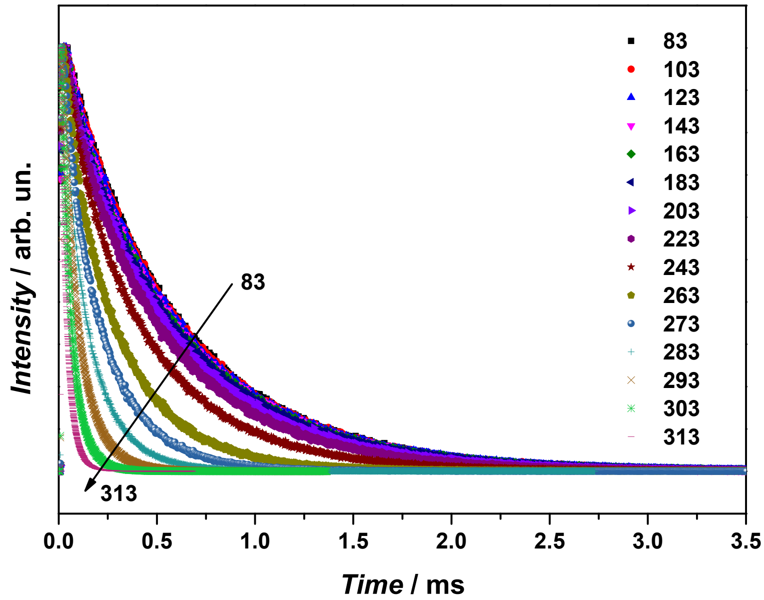

Figure S13: Temperature dependence of $^5D_4$ emitter state decay curves (λ_{ex} = 360 nm / λ_{em} = 545 nm).

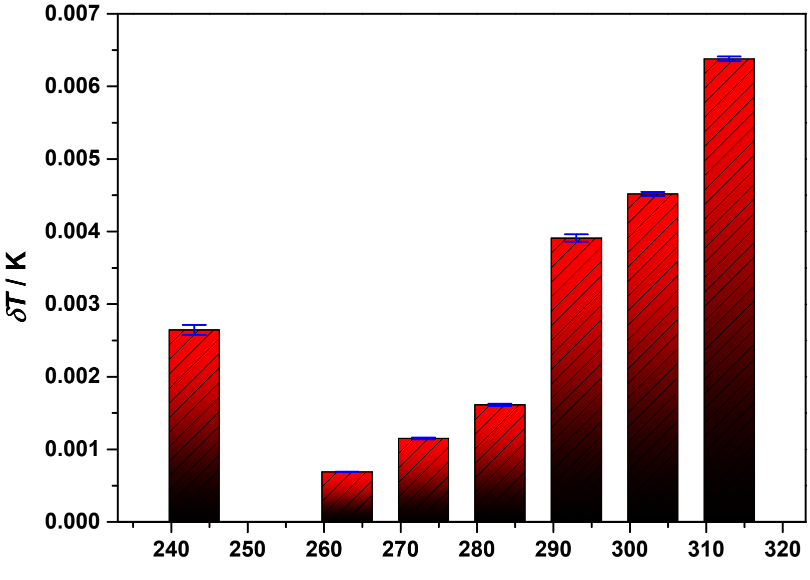

Figure S14: Temperature uncertainty for lifetime-based thermometry of the $[Tb(bzac)_3(H_2O)_2]$ complex.

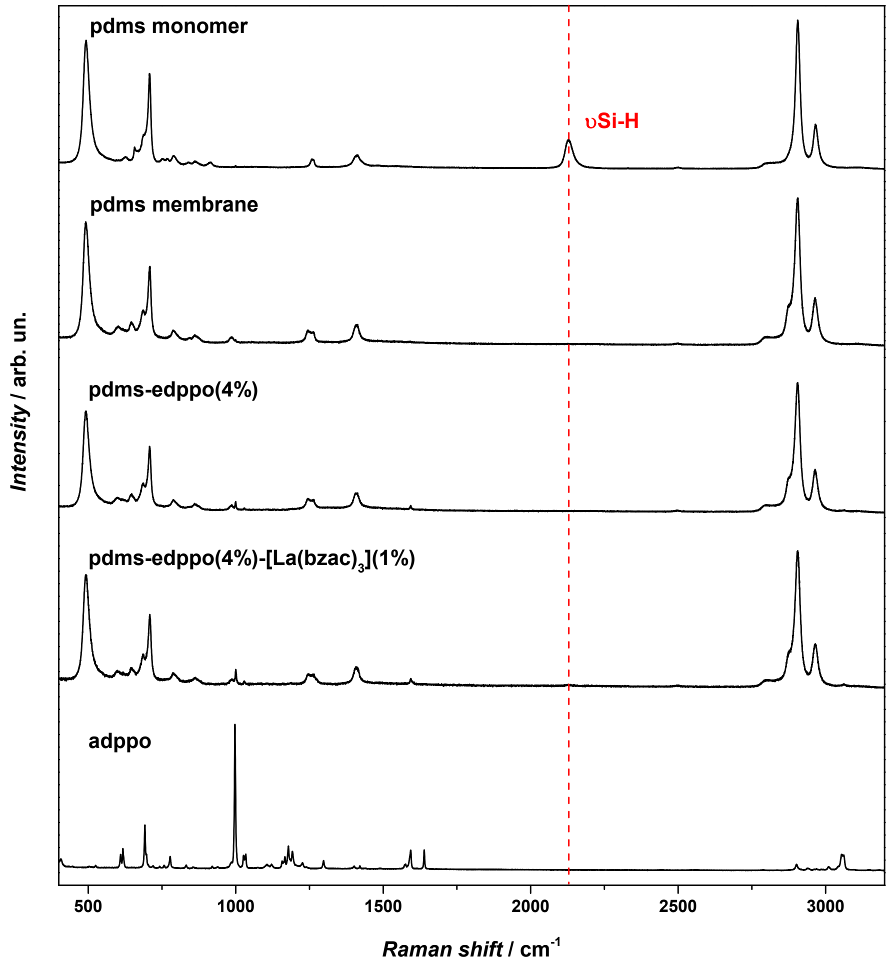

Figure S15: Raman spectra of some systems.

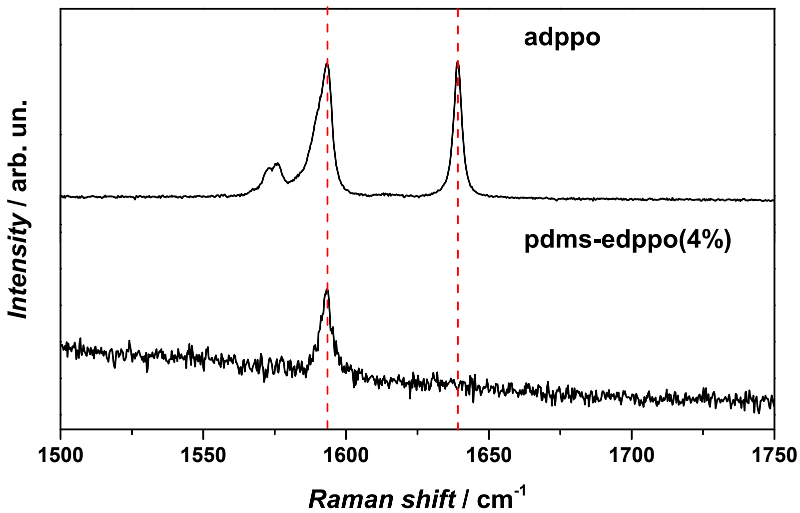

Figure 16: Magnification of the 1500-1750 cm^{-1} region of the Raman spectra of the adppo and pdms-edppo(4%).

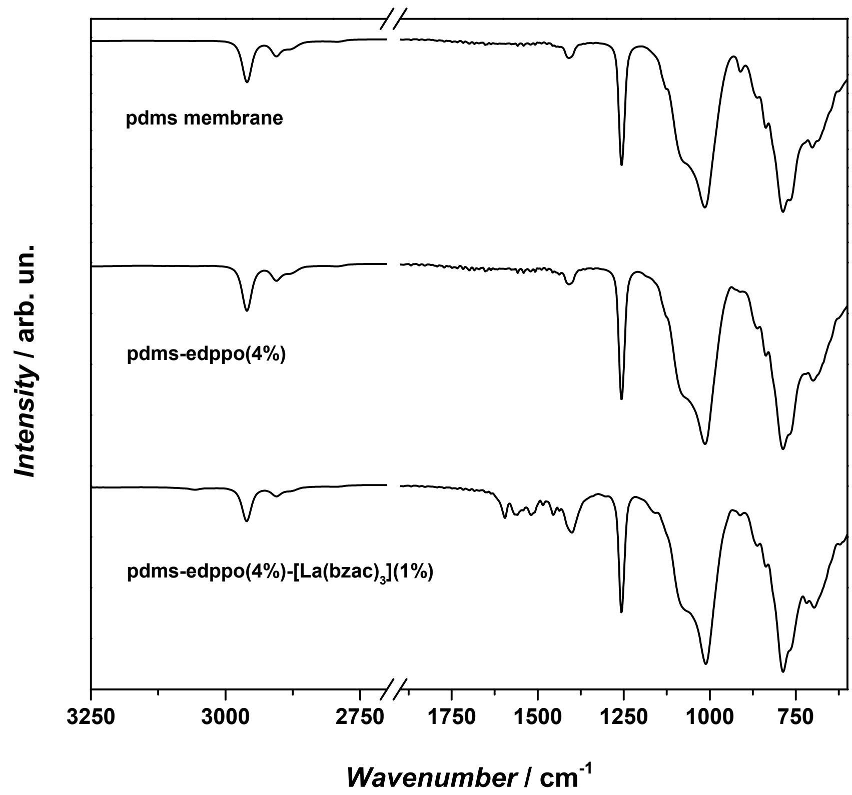

Figure S17: FTIR spectra of some systems.

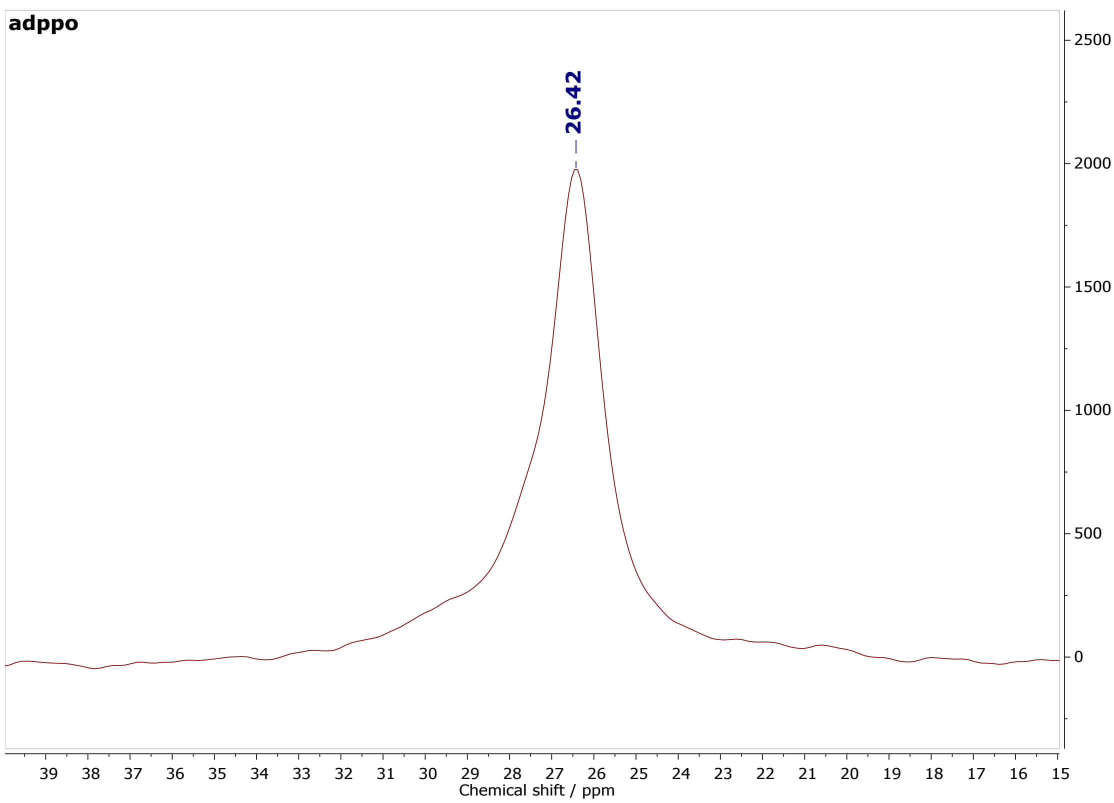

Figure S18: ^{31}P NMR spectra of adppo compound.

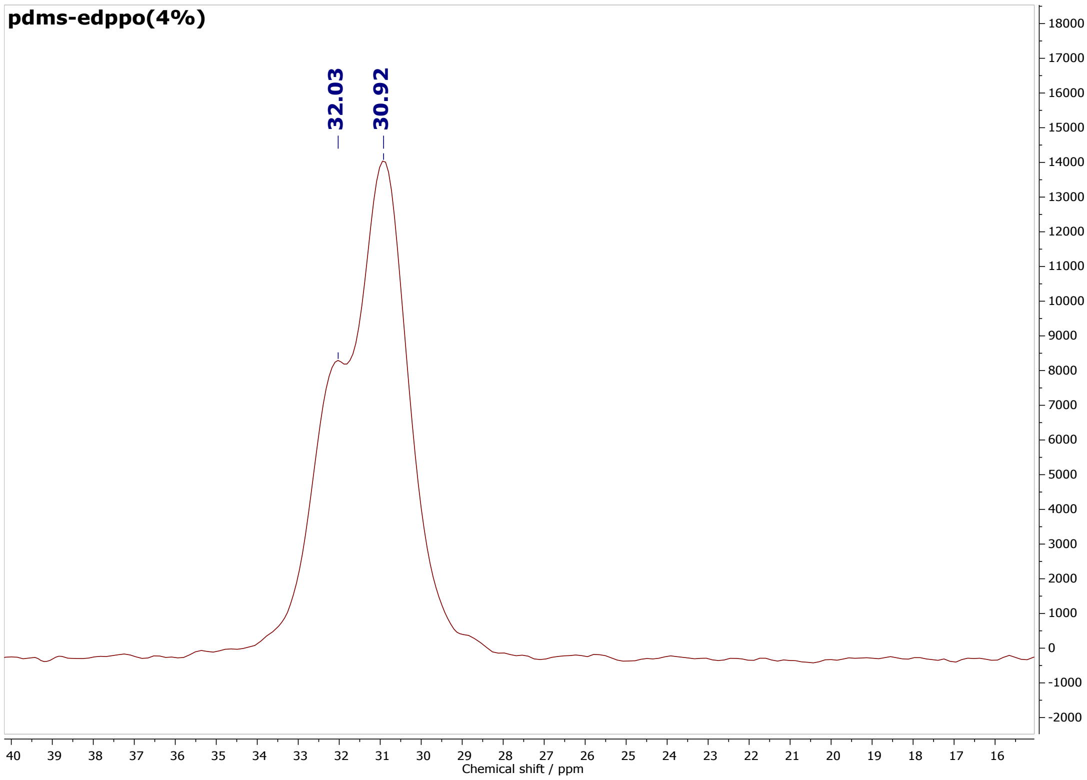

Figure S19: ^{31}P NMR spectra of pdms-edppo(4%) membrane.

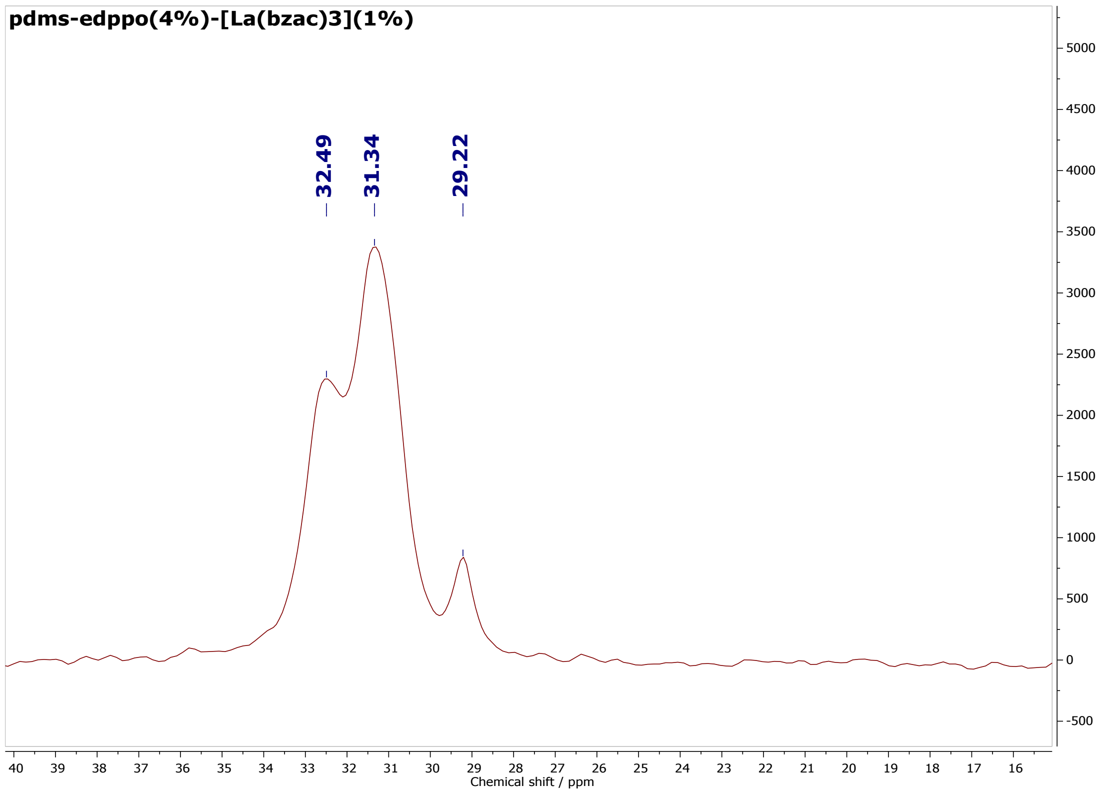

Figure S20: ^{31}P NMR spectra of pdms-edppo(4%)-[La(bzac)$_3$](1%) membrane.

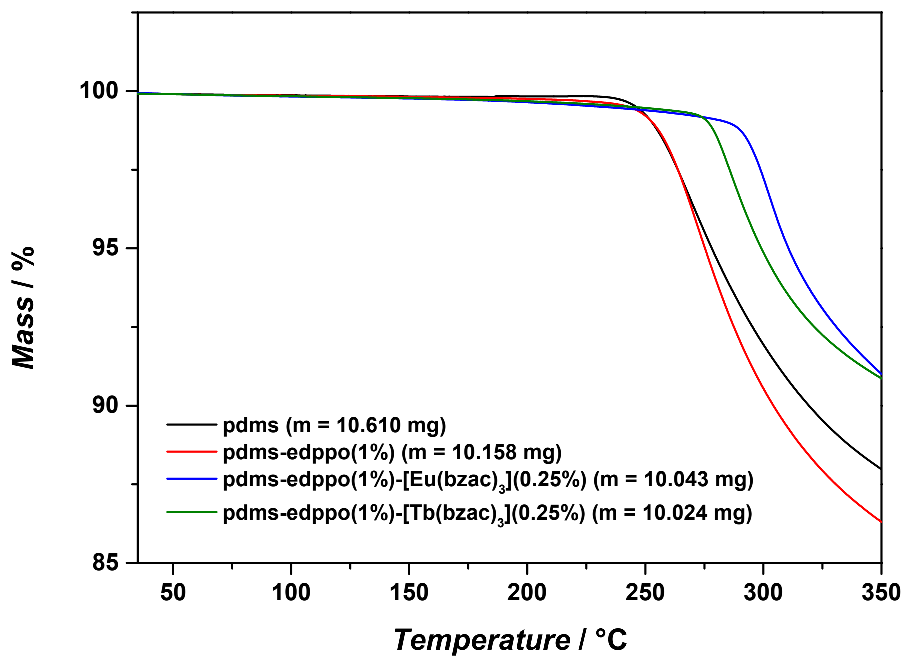

Figure S21: Thermogravimetric curves of some membranes.

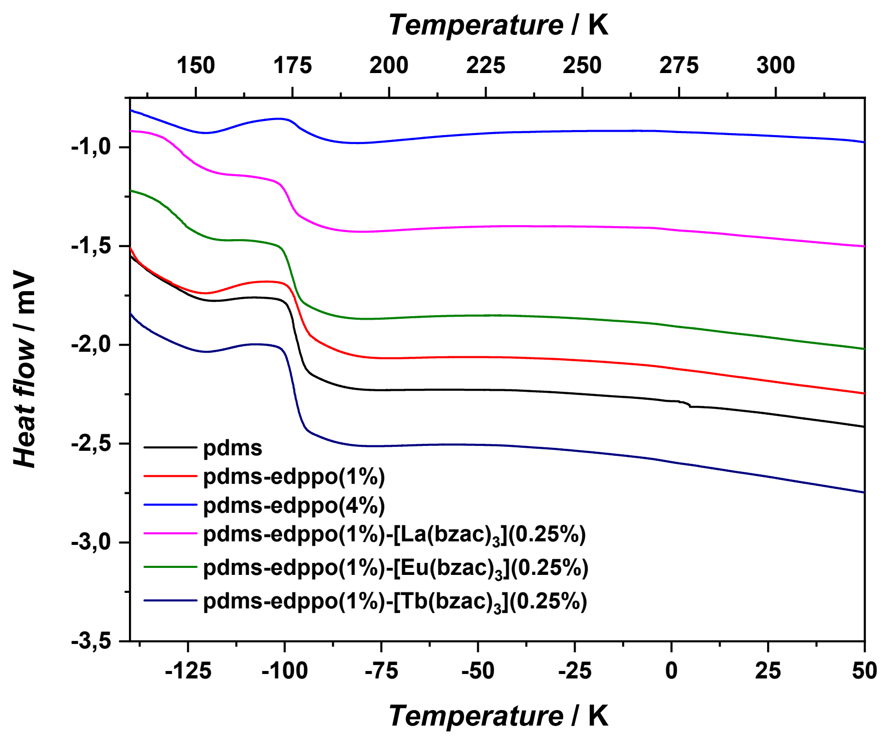

Figure S22: DSC curves of some membranes.

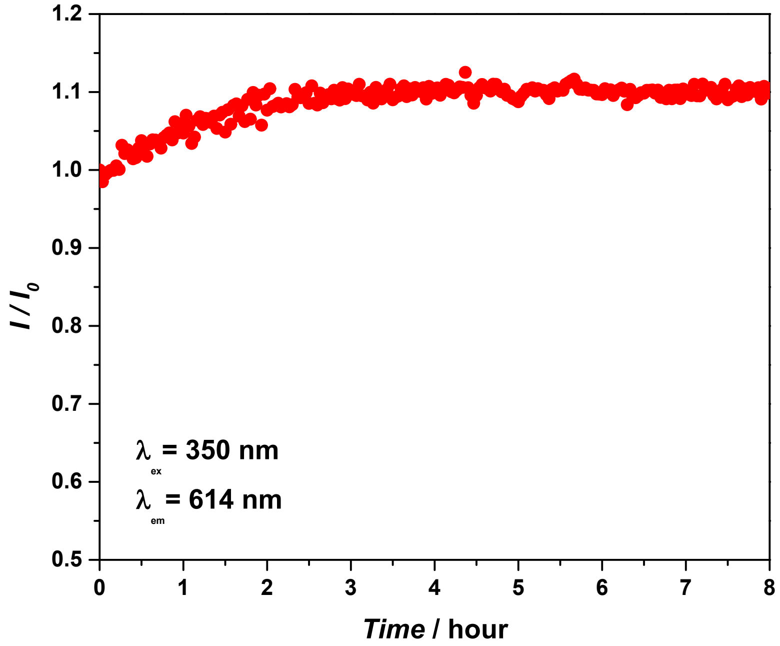

Figure S23: Photostability study of pdms-edppo(1%)-[Eu(bzac)$_3$](0.25%) membrane in air atmosphere.

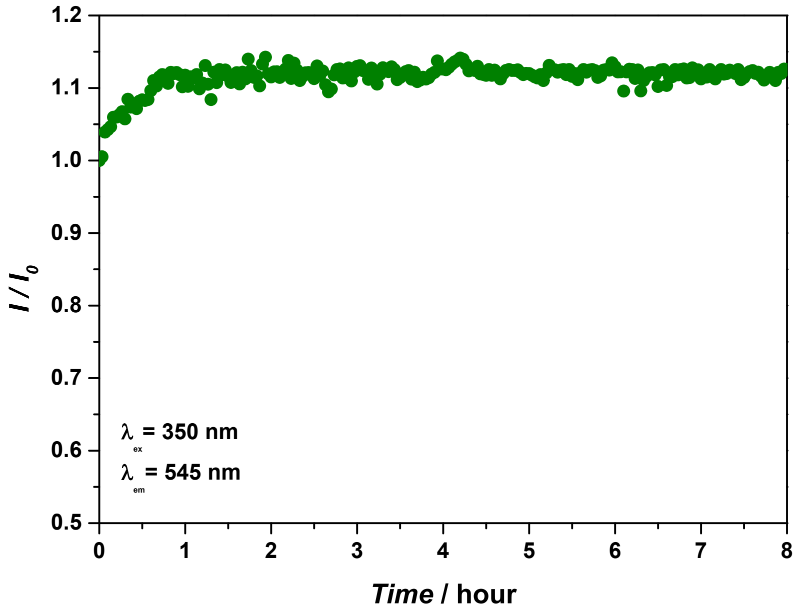

Figure S24: Photostability study of pdms-edppo(1%)-[Tb(bzac)$_3$](0.25%) membrane in air atmosphere.

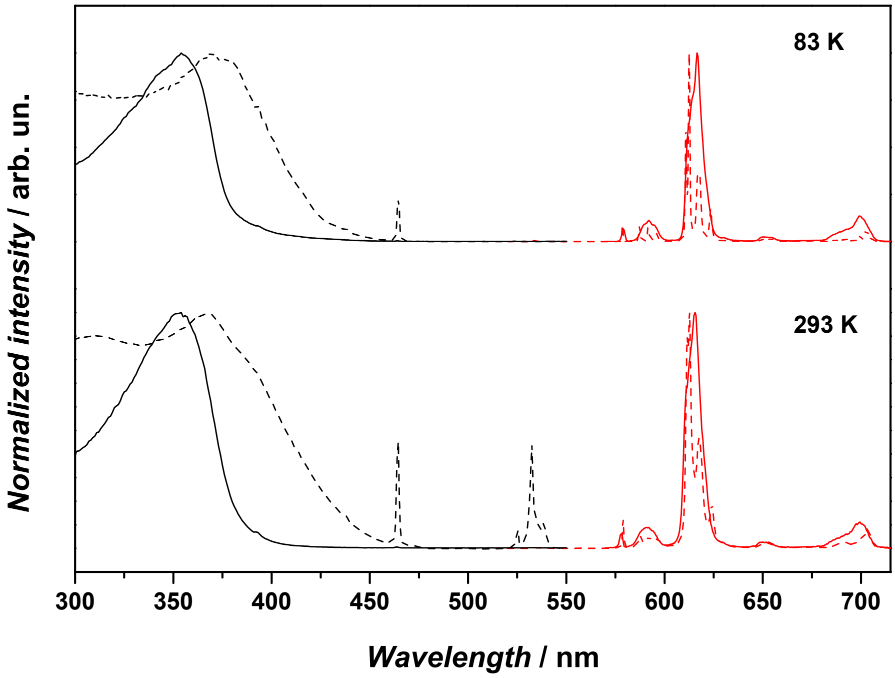

Figure S25: Excitation (black line) and emission (red line) of pdms-edppo(1%)-[Eu(bzac)$_3$](0.25%) membrane (solid line) and [Eu(bzac)$_3$(H_2O)$_2$] complex (dashed line) at 83 and 293 K. Bands assignment follow those of Figure S5.

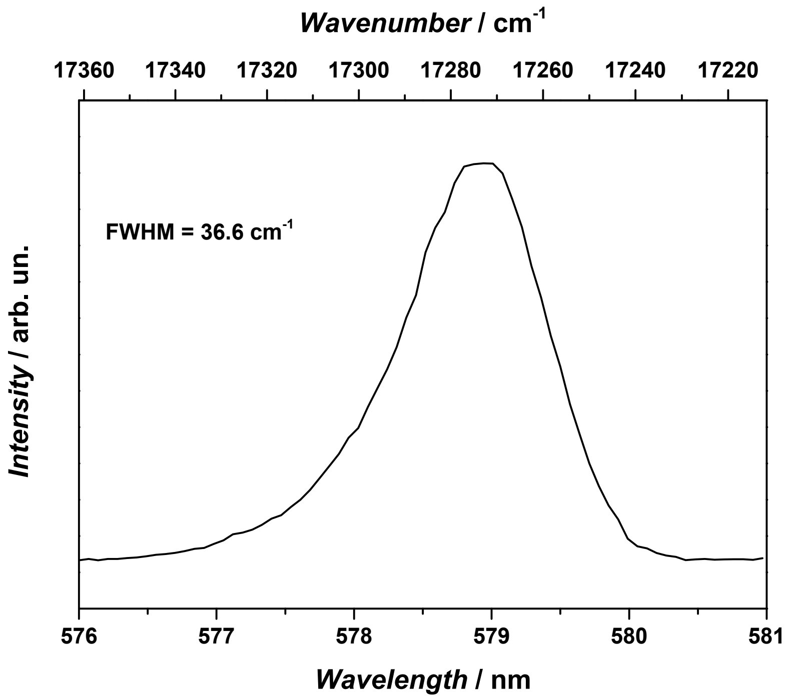

Figure S26: High resolution spectra obtained at 83 K of the $^5D_0 \rightarrow {}^7F_0$ transition band for the pdms-edppo(1%)-[Eu(bzac)$_3$](0.25%) membrane.

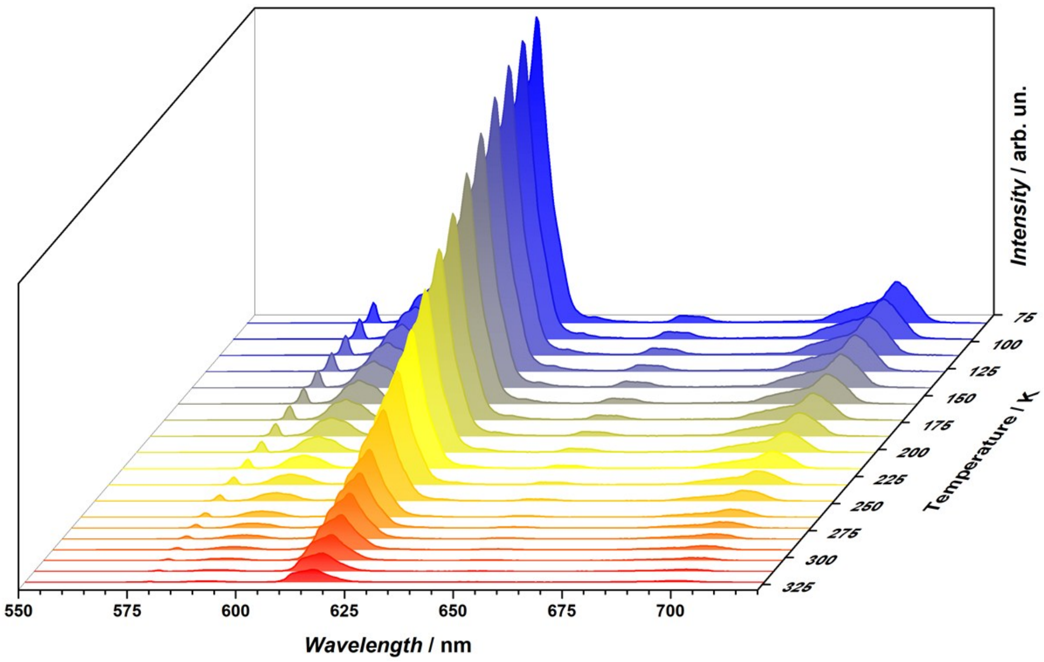

Figure S27: Temperature dependence of the emission spectra of pdms-edppo(1%)-[Eu(bzac)$_3$](0.25%) membrane.

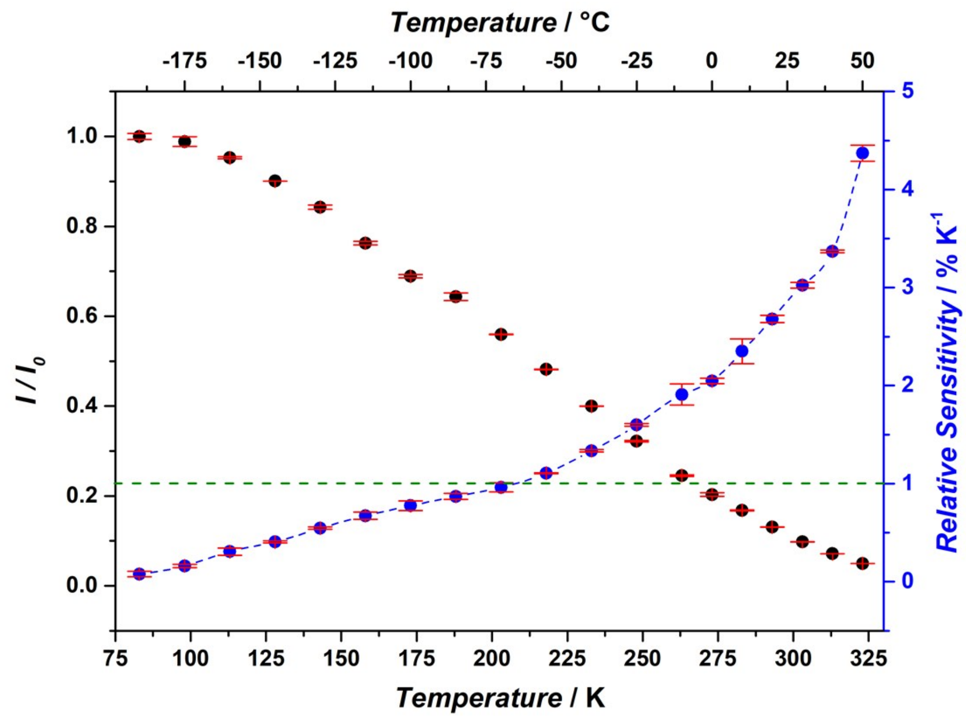

Figure S28: Temperature dependence of the integrated area of the $^5D_0 \rightarrow {}^7F_2$ transition band of the pdms-edppo(1%)-[Eu(bzac)$_3$](0.25%) membrane (black point) and the relative sensitivity obtained (blue point); green line is only a guide for the eyes indicating the relative sensitivity of 1 % K^{-1}.

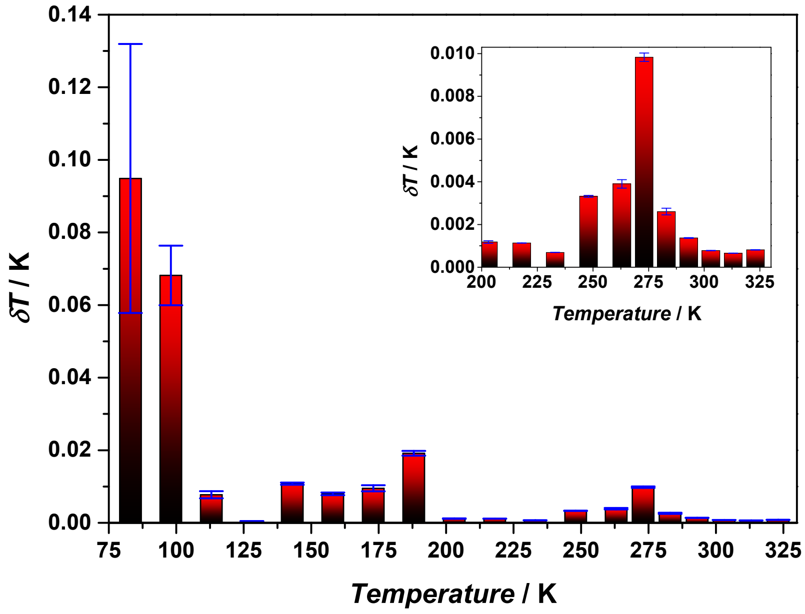

Figure S29: Temperature uncertainty at the temperature probing for the pdms-edppo(1%)-[Eu(bzac)$_3$](0.25%) membrane (inset: magnification of the signals in the operational temperature range).

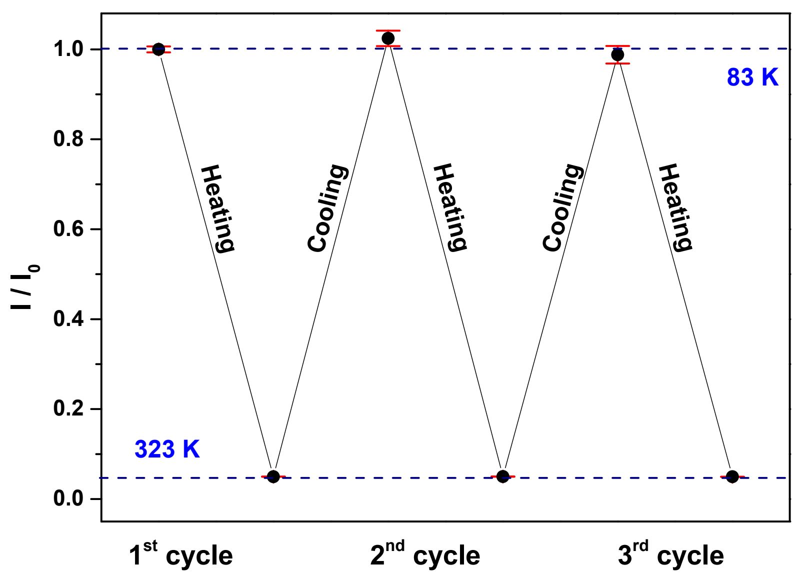

Figure S30: Thermal cycling for the pdms-edppo(1%)-[Eu(bzac)$_3$](0.25%) membrane.

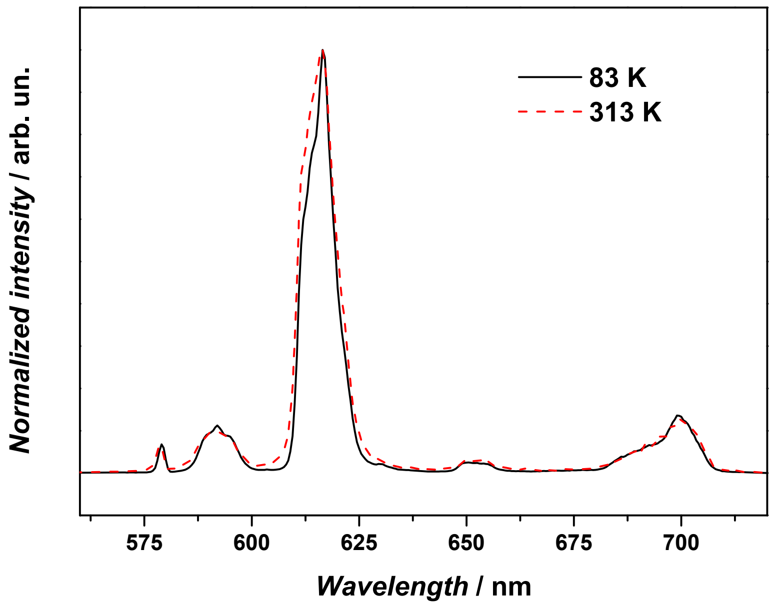

Figure S31: Comparison between 83 and 313 K emission spectra of pdms-edppo(1%)-[Eu(bzac)$_3$](0.25%) membrane.

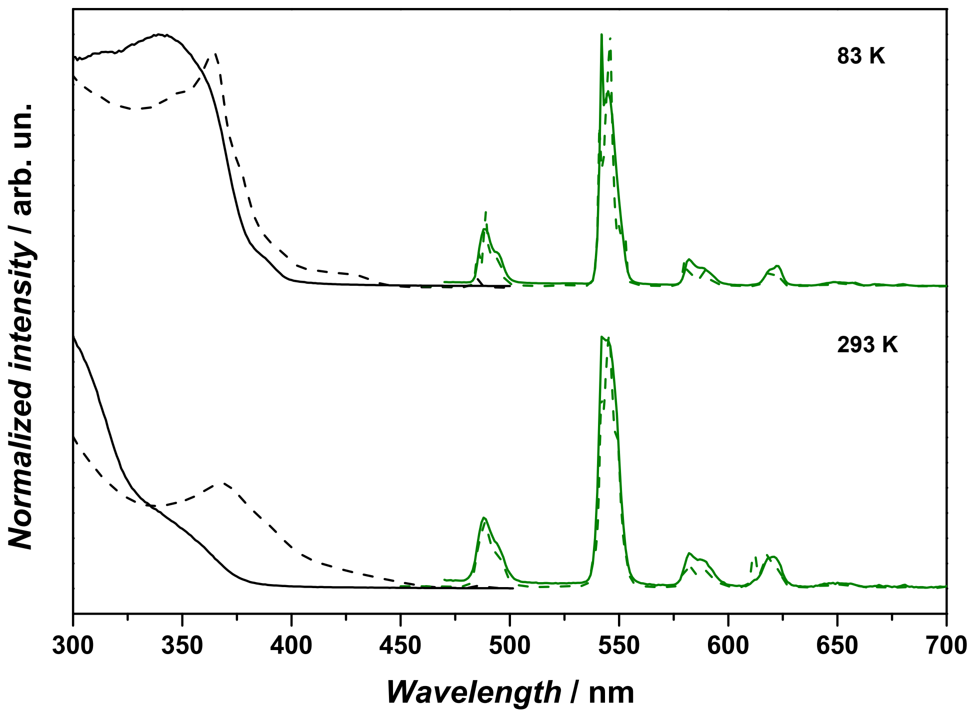

Figure S32: Excitation (black line) and emission (green line) of pdms-edppo(1%)-[Tb(bzac)$_3$](0.25%) membrane (solid line) and [Tb(bzac)$_3$(H$_2$O)$_2$] complex (dashed line) at 83 and 293 K. Bands assignment follow those of Figure S6.

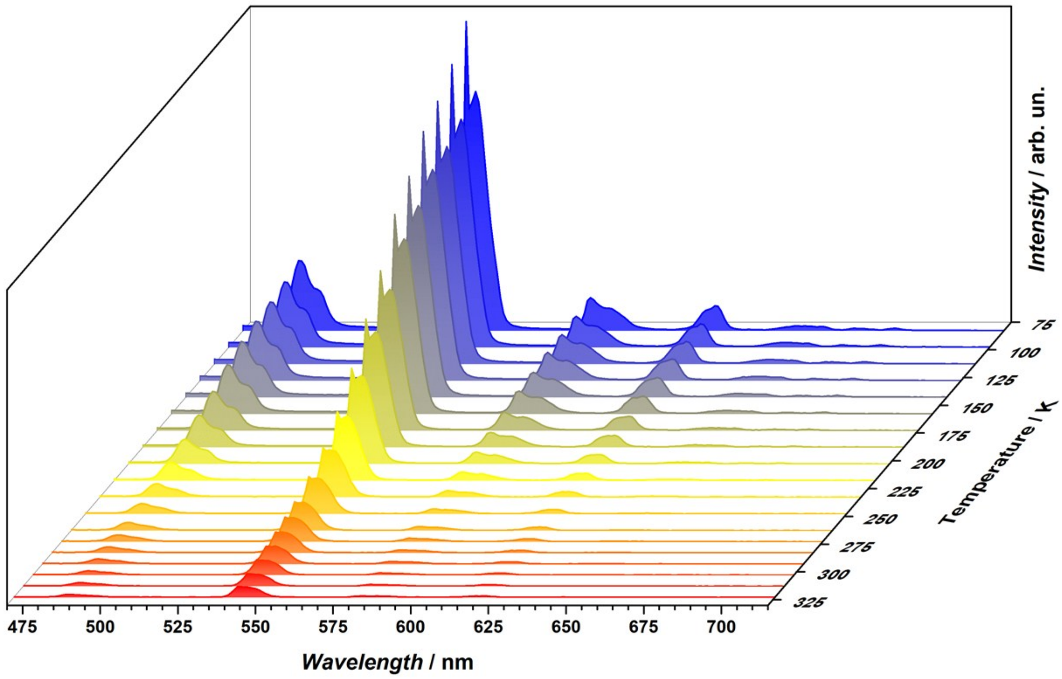

Figure S33: Temperature dependence of the emission spectra of pdms-edppo(1%)-[Tb(bzac)$_3$](0.25%) membrane. Bands assignment follow those of Figure 1-a.

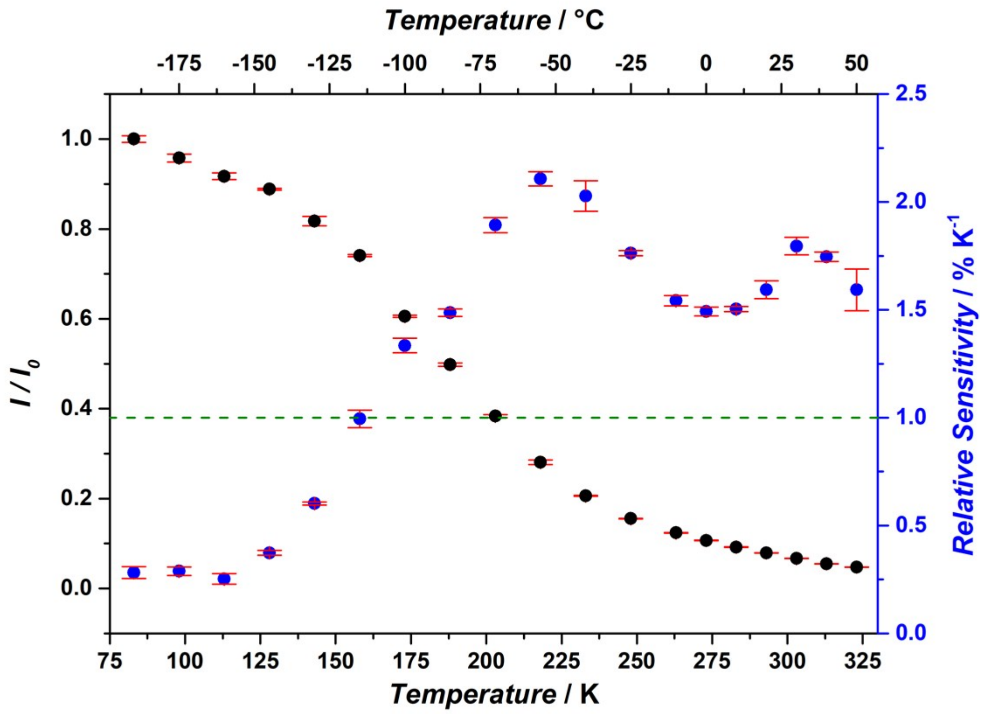

Figure S34: Temperature dependence of the integrated area of the $^5D_4 \rightarrow {}^7F_5$ transition band of the pdms-edppo(1%)-[Tb(bzac)$_3$](0.25%) membrane (black point) and the relative sensitivity obtained (blue point); green line is only a guide for the eyes indicating the relative sensitivity of 1 % K^{-1}.

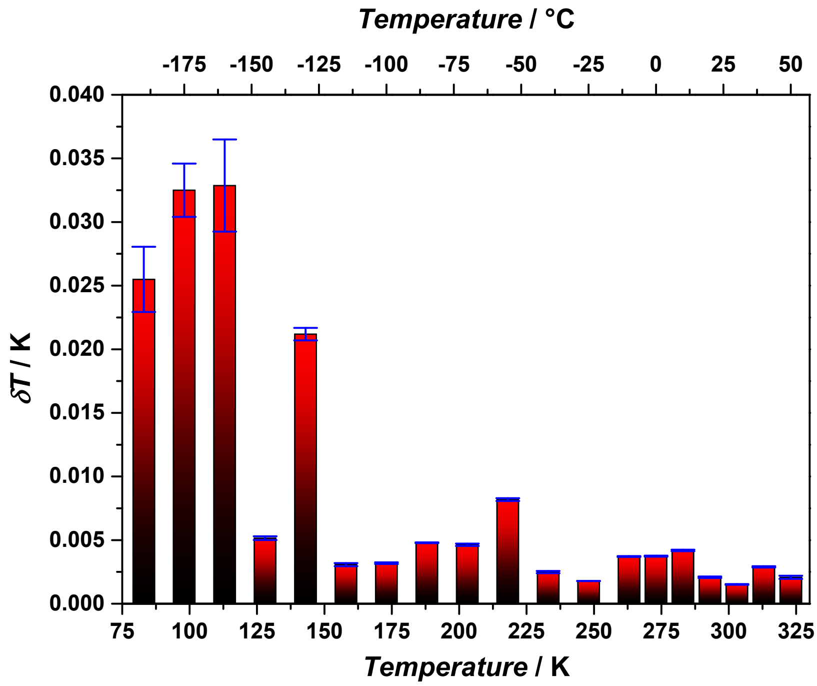

Figure S35: Temperature uncertainty at the temperature probing for the pdms-edppo(1%)-[Tb(bzac)$_3$](0.25%) membrane.

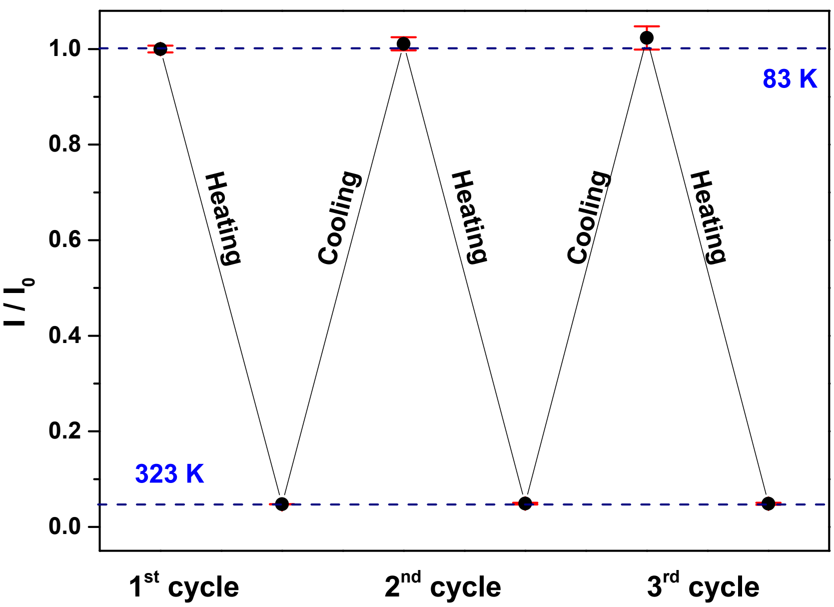

Figure S36: Thermal cycling for the pdms-edppo(1%)-[Tb(bzac)$_3$](0.25%) membrane.

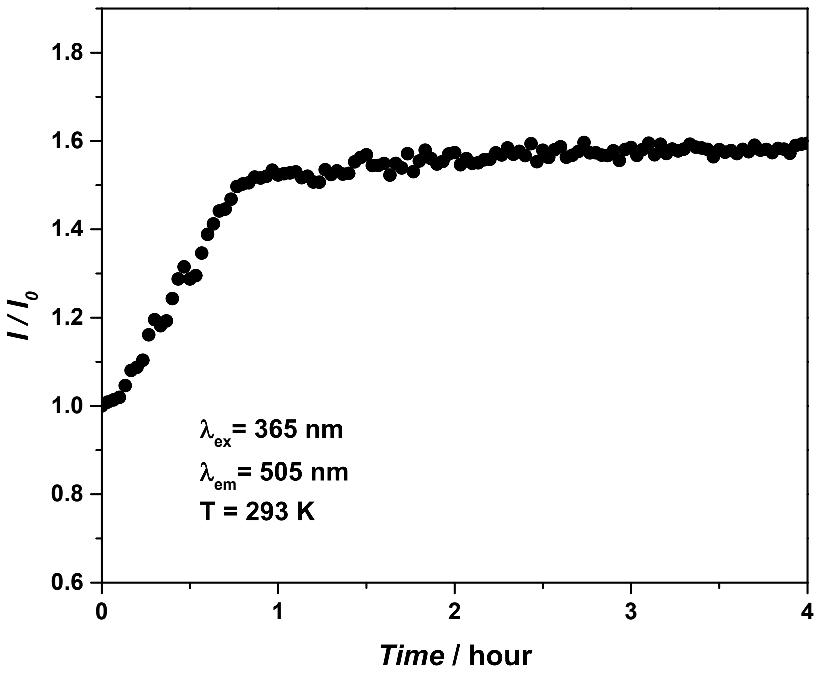

Figure S37: Photostability study of pdms-edppo(1%)-[Gd(bzac)$_3$](0.25%) membrane in air atmosphere.

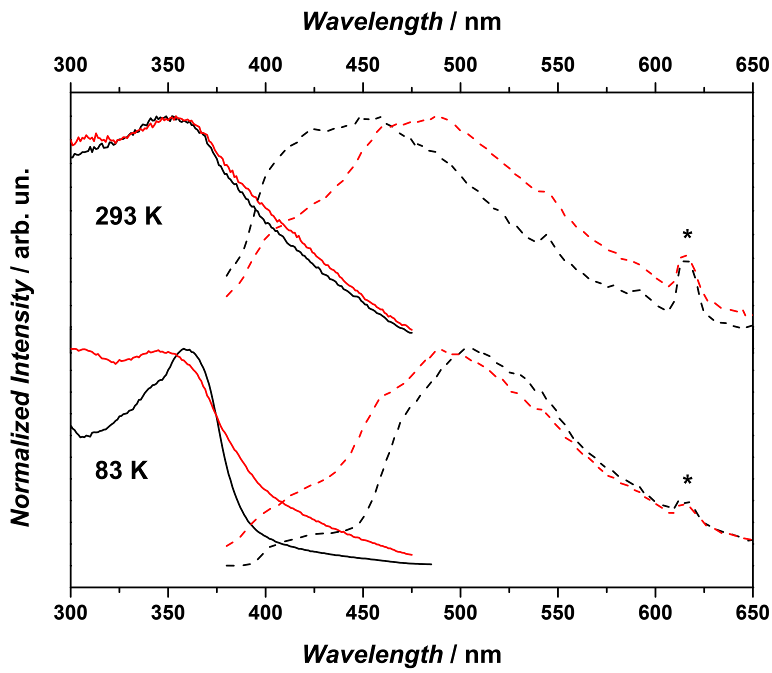

Figure S38: Comparison between 83 and 293 K excitation, λ_{em} = 505 nm, (full line) and emission, λ_{ex} = 365 nm, (dashed line) for the pdms-edppo(1%)-[Gd(bzac)$_3$](0.25%) membrane before (black line) and after (red line) the activation step. * indicates a commonly europium(III) contamination even in high purity gadolinium(III) oxide.

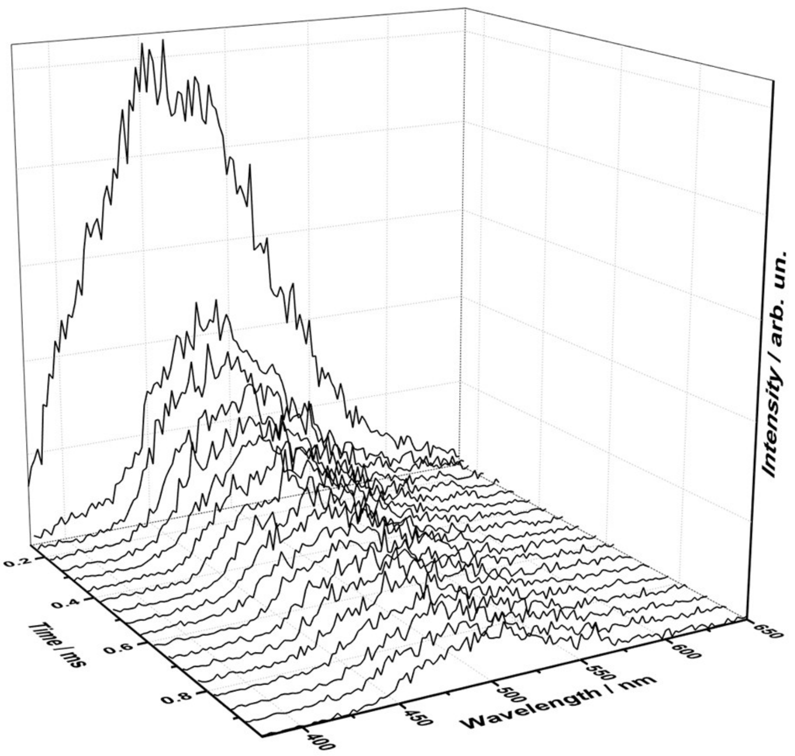

Figure S39: Time-resolved emission spectra (λ_{ex} = 365 nm) for the pdms-edppo(1%)-[Gd(bzac)$_3$](0.25%) membrane at 83 K.

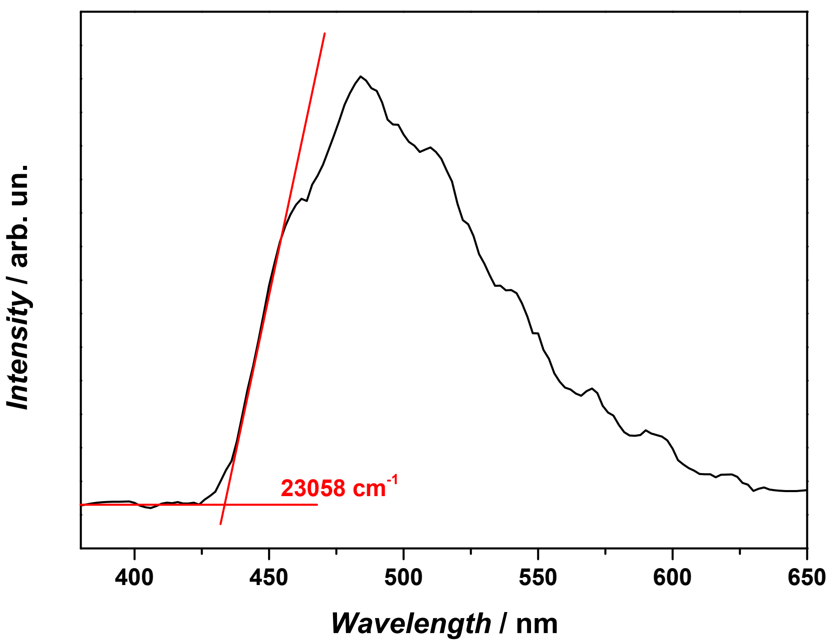

Figure S40: Emission spectra (λ_{ex} = 365 nm) for the pdms-edppo(1%)-[Gd(bzac)$_3$](0.25%) membrane at 83 K with 0.62 ms delay.

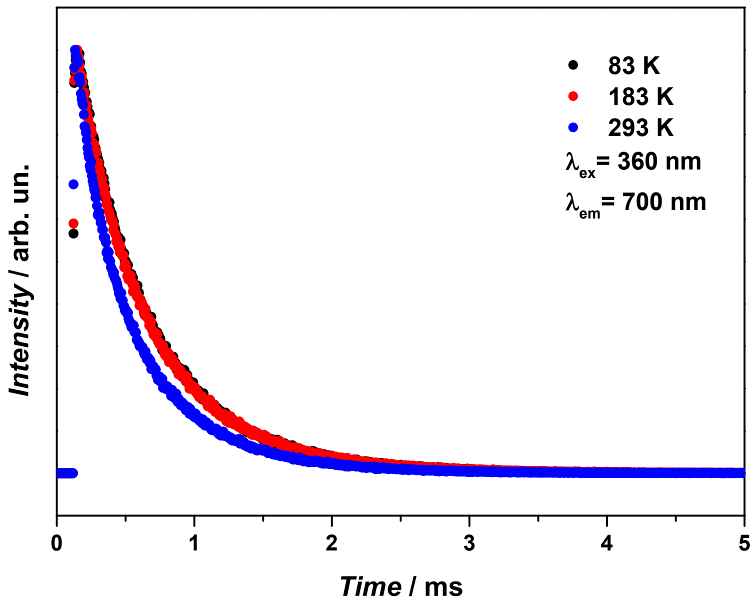

Figure S41: Decay curves of the $^5D_0$ emitter state for the pdms-edppo(1%)-[Eu(bzac)$_3$](0.25%) membrane.

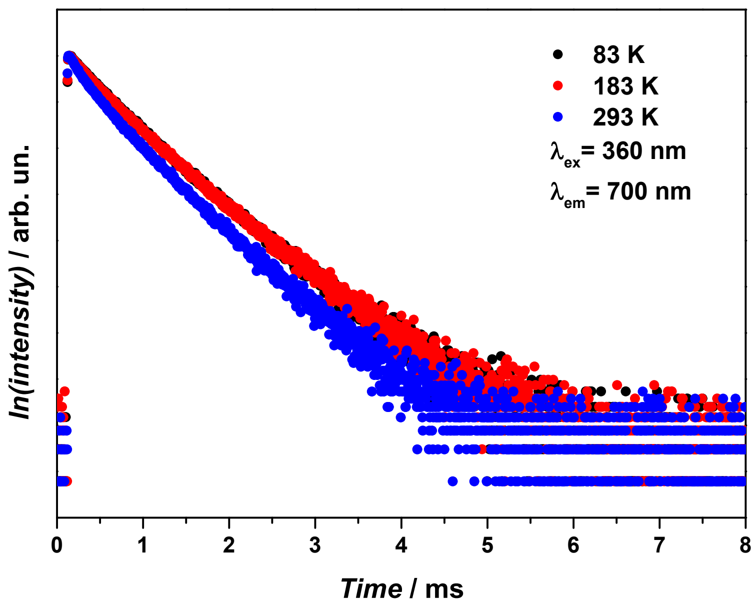

Figure S42: Linearization of the decay curves of the $^5D_0$ emitter state for the pdms-edppo(1%)-[Eu(bzac)$_3$](0.25%) membrane.

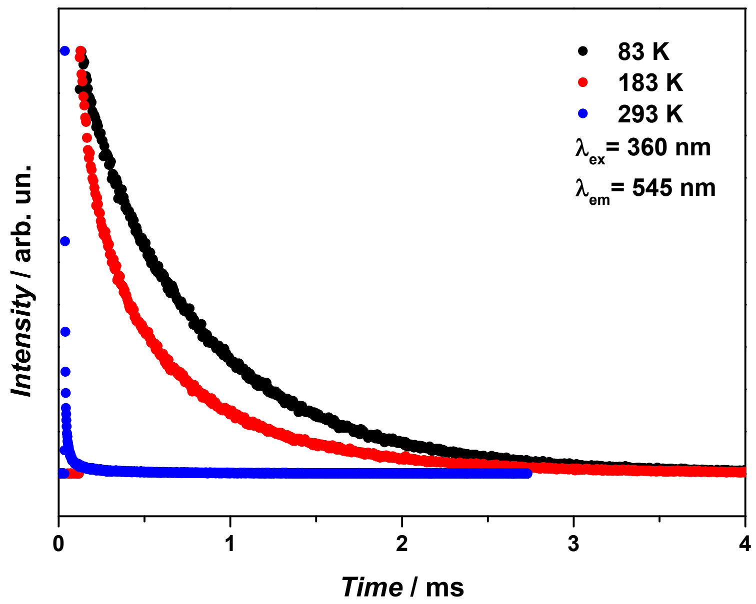

Figure S43: Decay curves of the $^5D_4$ emitter state for the pdms-edppo(1%)-[Tb(bzac)$_3$](0.25%) membrane.

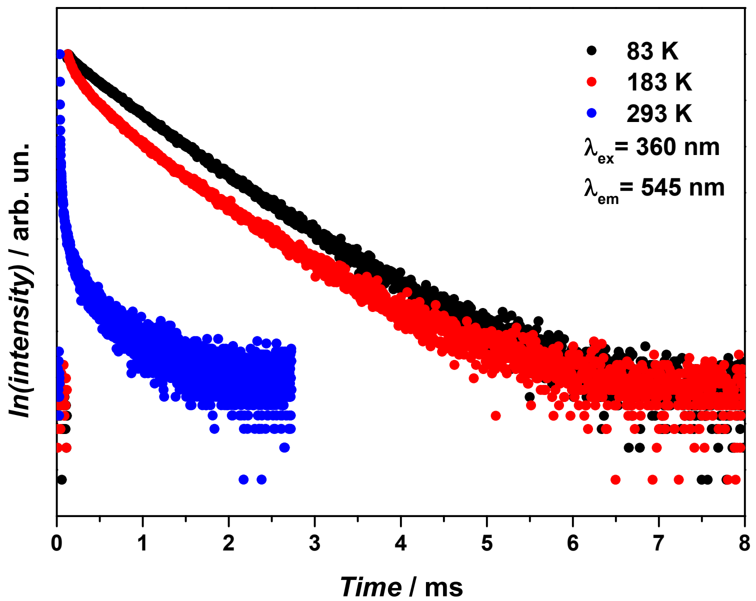

Figure S44: Linearization of the decay curves of the $^5D_4$ emitter state for the pdms-edppo(1%)-[Tb(bzac)$_3$](0.25%) membrane.

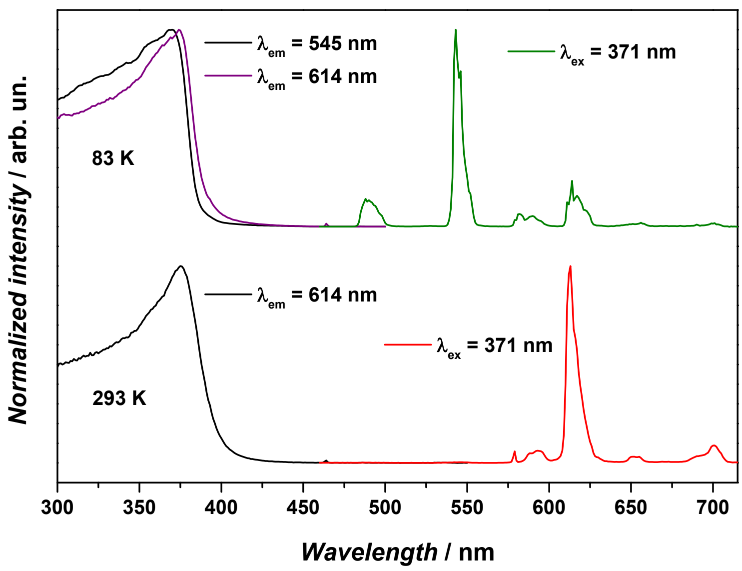

Figure S45: Excitation and emission of the pdms-eddpo(1%)-[$Tb_{0.90}Eu_{0.10}(bzac)_3$](0.25%) membrane at 83 and 293 K.

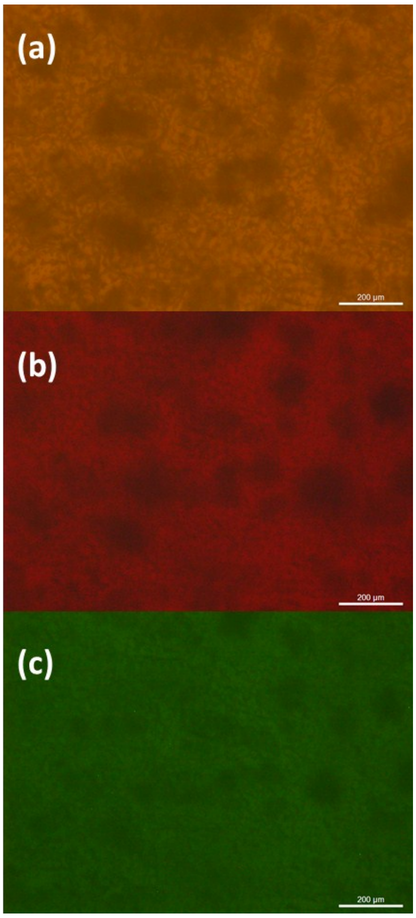

Figure S46: Images of the pdms-eddpo(1%)-[$Tb_{0.90}Eu_{0.10}(bzac)_3$](0.25%) membrane under white light (a) and epifluorescence images exciting at 350 nm obtained at 293 K (b) and 77 K (c).

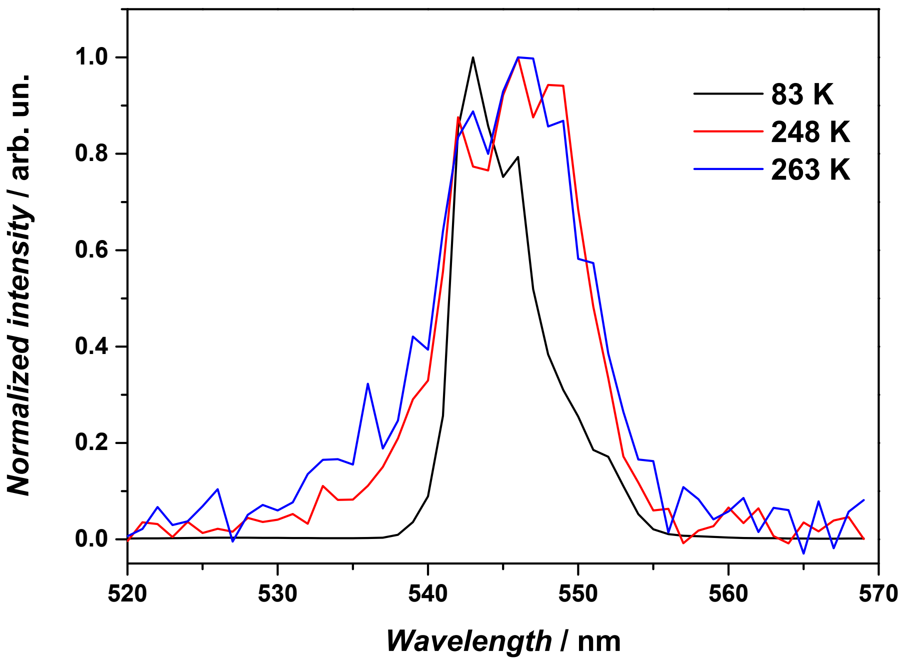

Figure S47: Comparison of the I_2 region of the emission spectra for pdms-eddpo(1%)-[$Tb_{0.90}Eu_{0.10}(bzac)_3$](0.25%) membrane at 83 248 and 263 K.

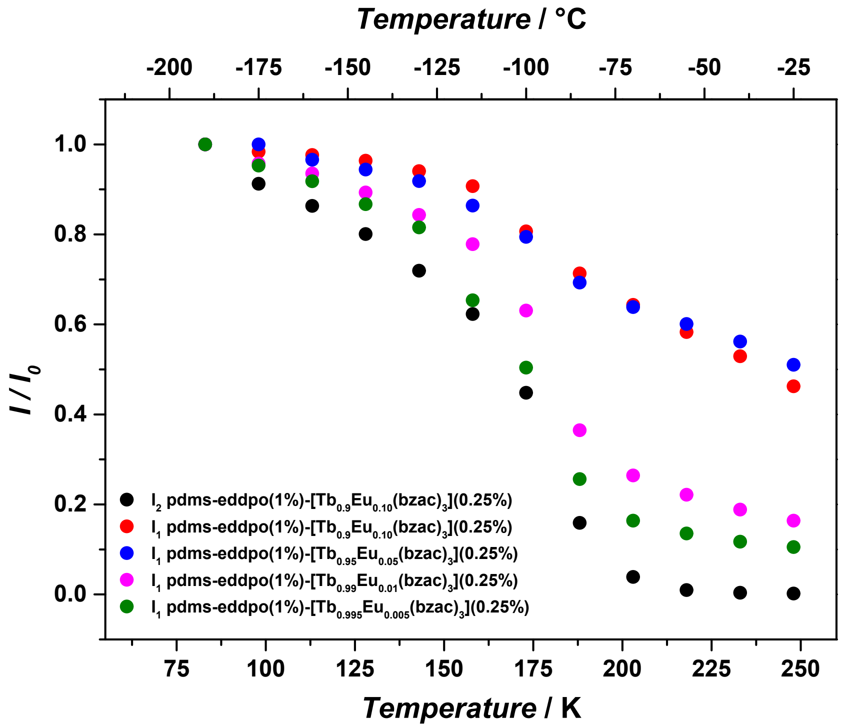

Figure S48: Temperature dependence of I_1 of the four ratiometric membranes compared with I_2 for pdms-eddpo(1%)-[$Tb_{0.90}Eu_{0.10}(bzac)_3$](0.25%) on the 83-243 K range.

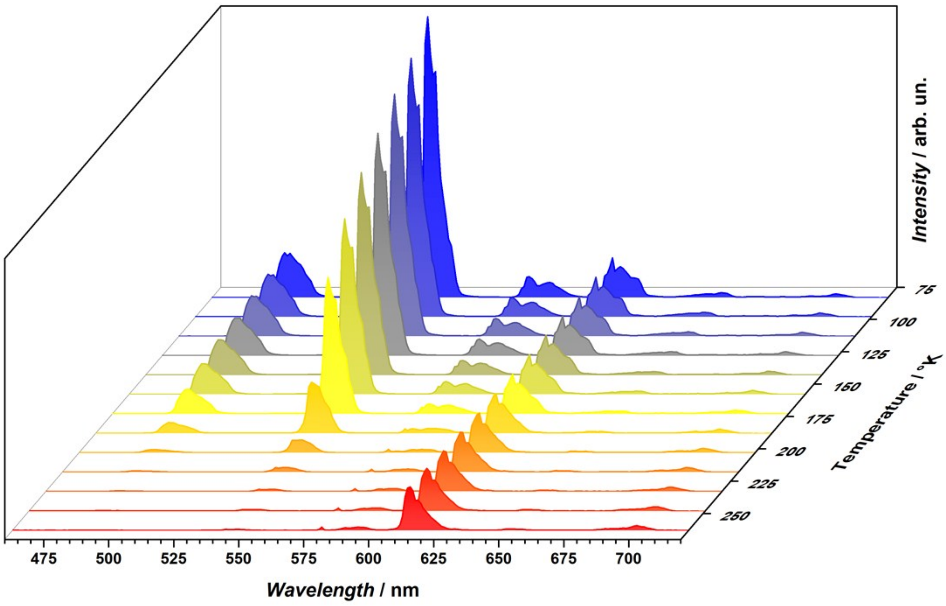

Figure S49: Temperature evolution of the emission spectra of pdms-eddpo(1%)-[$Tb_{0.95}Eu_{0.05}(bzac)_3$](0.25%) membrane (normalized to keep the europium $^5D_0 \rightarrow {}^7F_2$ transition band with a constant intensity). Bands assignment follow those of Figure 2-a.

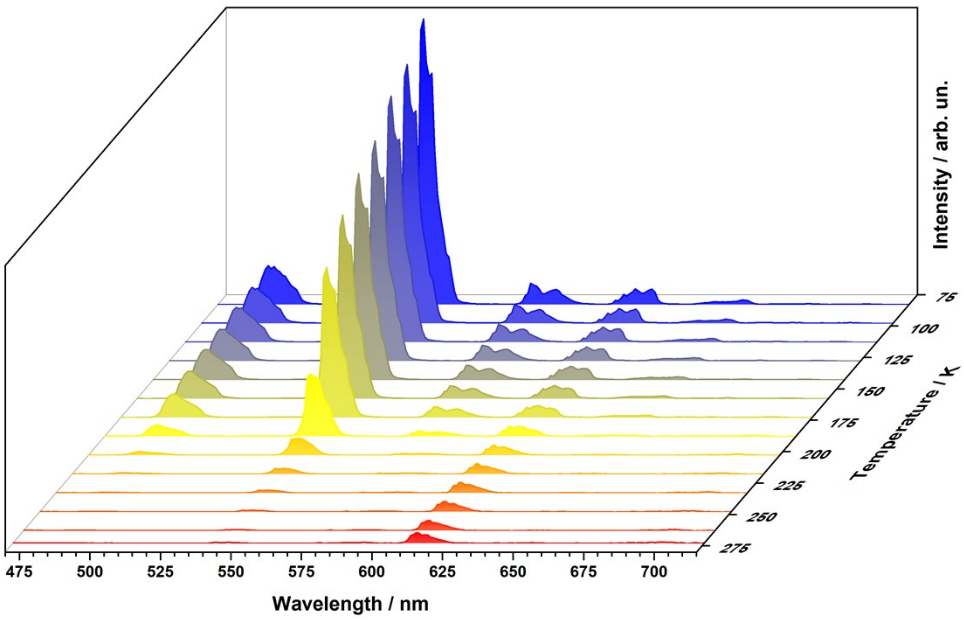

Figure S50: Temperature evolution of the emission spectra of pdms-eddpo(1%)-[$Tb_{0.99}Eu_{0.01}(bzac)_3$](0.25%) membrane (normalized to keep the europium $^5D_0 \rightarrow {}^7F_2$ transition band with a constant intensity). Bands assignment follow those of Figure 2-a.

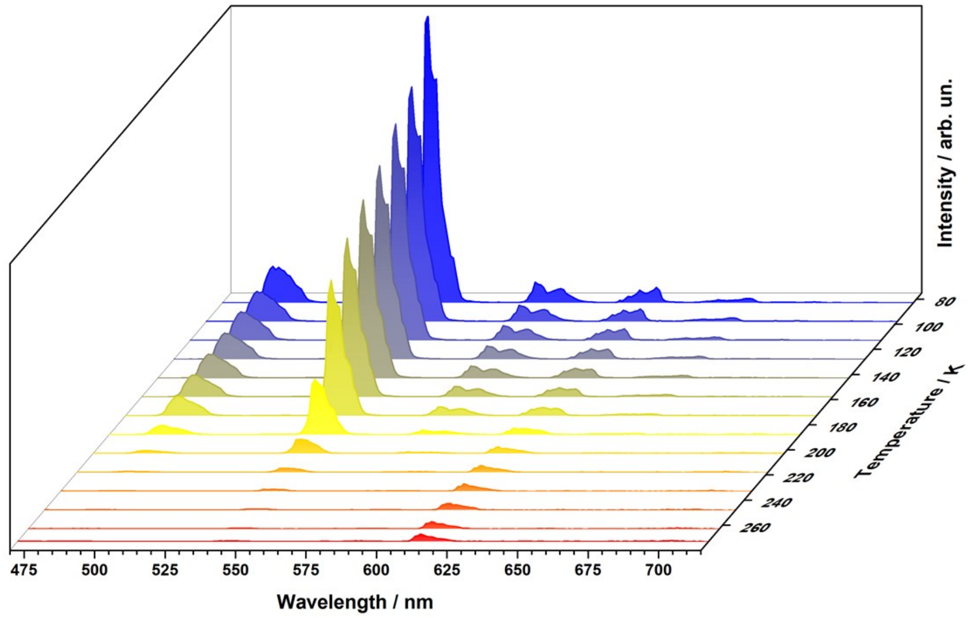

Figure S51: Temperature evolution of the emission spectra of pdms-eddpo(1%)-[$Tb_{0.995}Eu_{0.005}(bzac)_3$](0.25%) membrane (normalized to keep the europium $^5D_0 \rightarrow {}^7F_2$ transition band with a constant intensity). Bands assignment follow those of Figure 2-a.

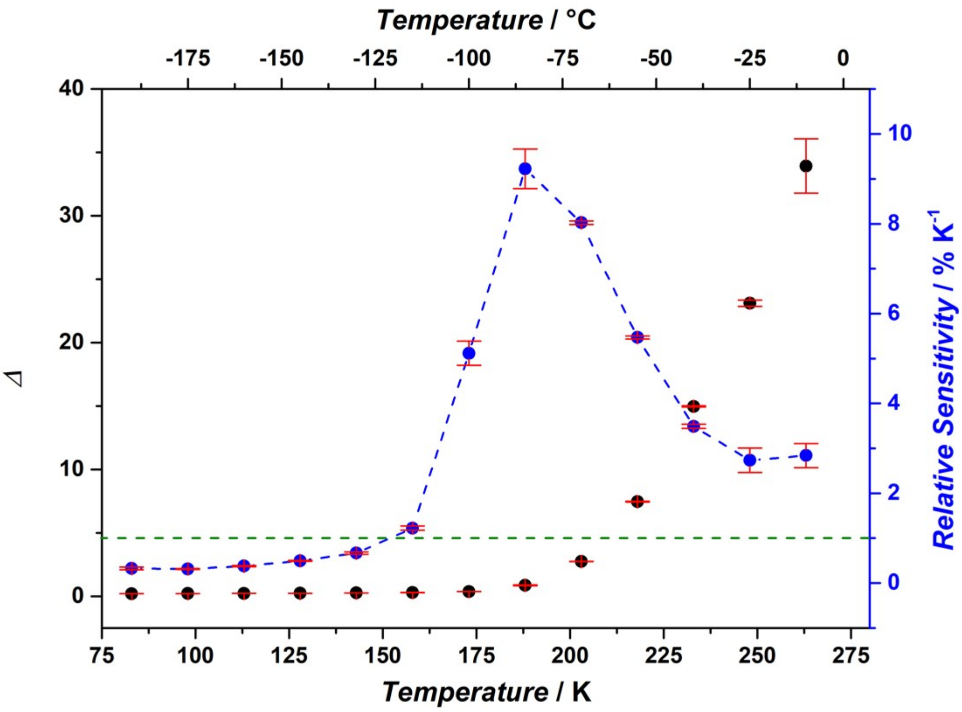

Figure S52: Temperature variation of Δ (black point) and the relative sensitivity obtained (blue point) of pdms-eddpo(1%)-[$Tb_{0.95}Eu_{0.05}(bzac)_3$](0.25%) membrane; green line is only a guide for the eyes indicating the relative sensitivity of 1 % K^{-1}.

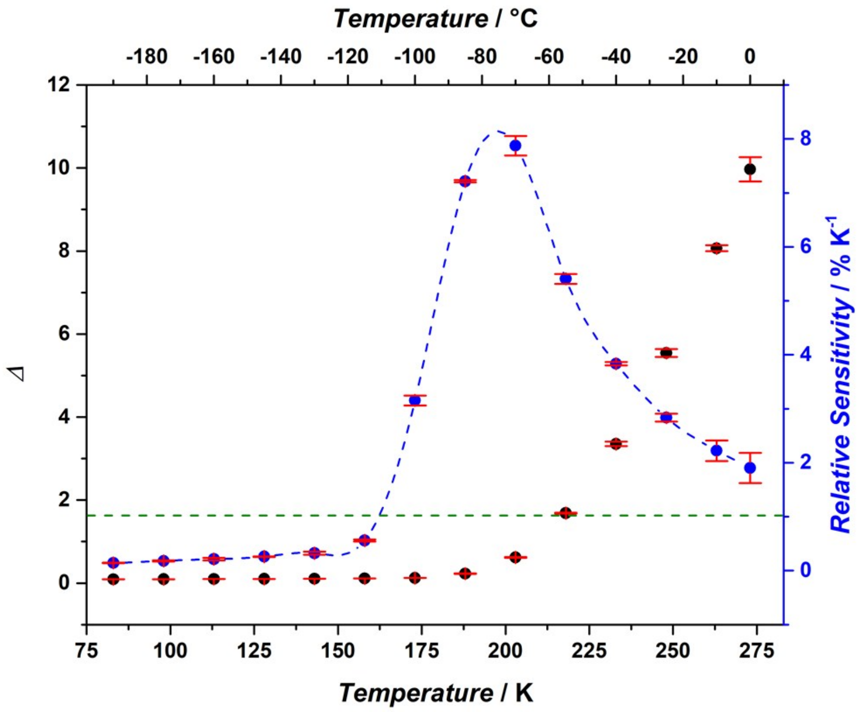

Figure S53: Temperature variation of Δ (black point) and the relative sensitivity obtained (blue point) of pdms-eddpo(1%)-[$Tb_{0.99}Eu_{0.01}(bzac)_3$](0.25%) membrane; green line is only a guide for the eyes indicating the relative sensitivity of 1 % K^{-1}.

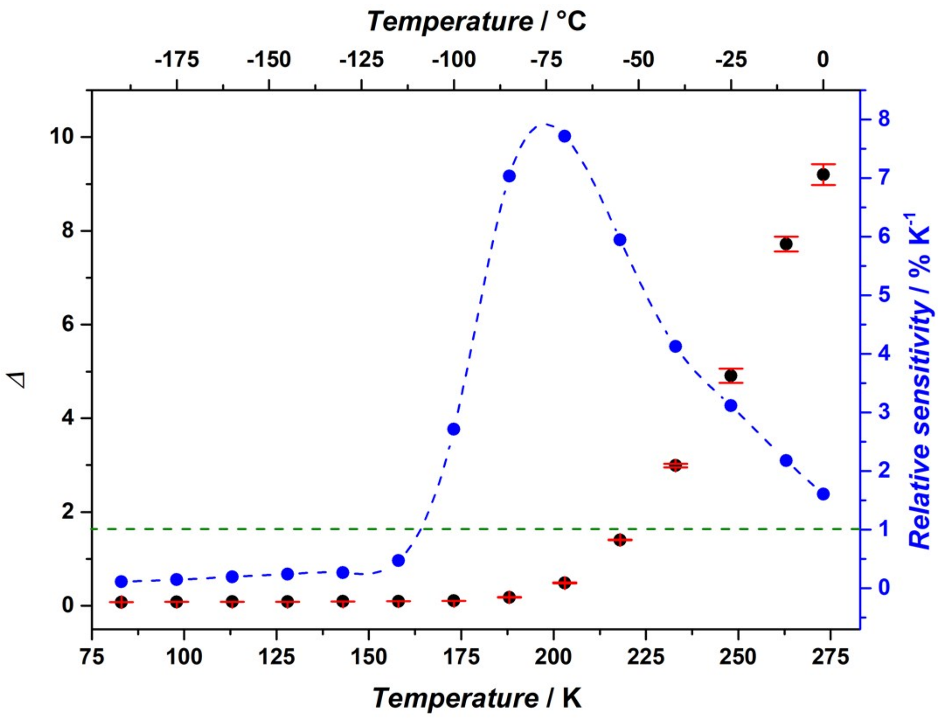

Figure S54: Temperature variation of Δ (black point) and the relative sensitivity obtained (blue point) of pdms-eddpo(1%)-[$Tb_{0.995}Eu_{0.005}(bzac)_3$](0.25%) membrane; green line is only a guide for the eyes indicating the relative sensitivity of 1 % K^{-1}.

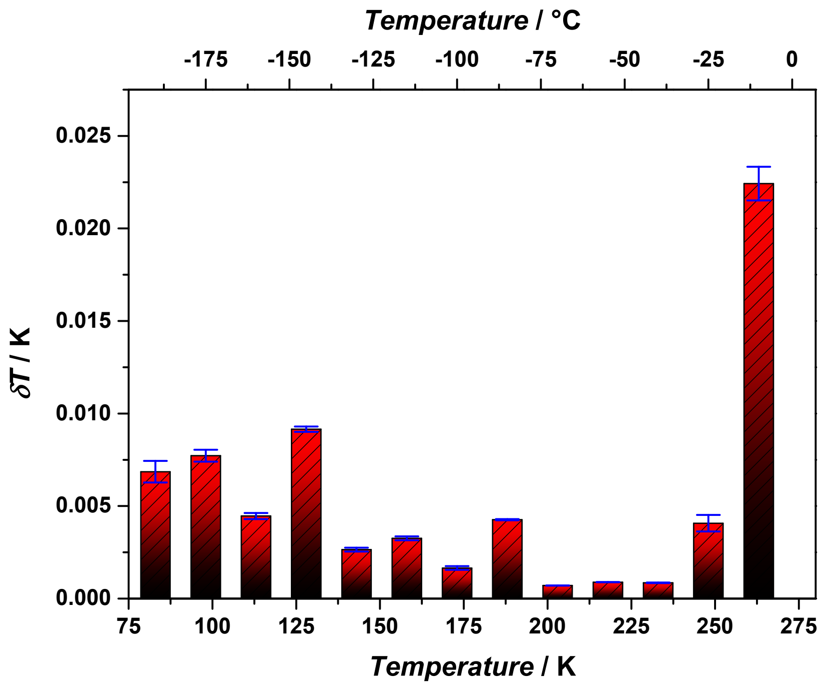

Figure S55: Temperature uncertainty for the pdms-eddpo(1%)-[$Tb_{0.95}Eu_{0.05}(bzac)_3$](0.25%) membrane.

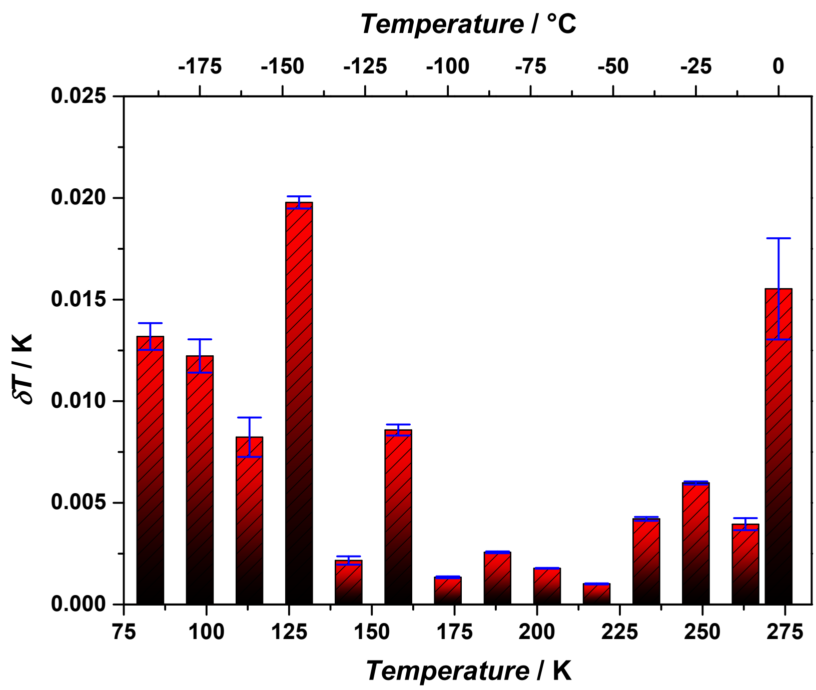

Figure S56: Temperature uncertainty for the pdms-eddpo(1%)-[$Tb_{0.99}Eu_{0.01}(bzac)_3$](0.25%) membrane.

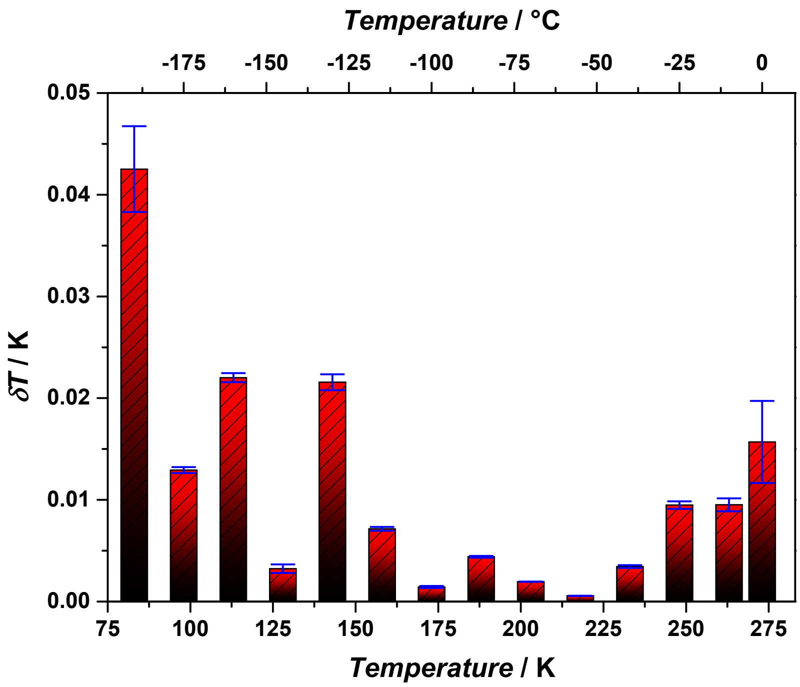

Figure S57: Temperature uncertainty for the pdms-eddpo(1%)-[$Tb_{0.995}Eu_{0.005}(bzac)_3$](0.25%) membrane.

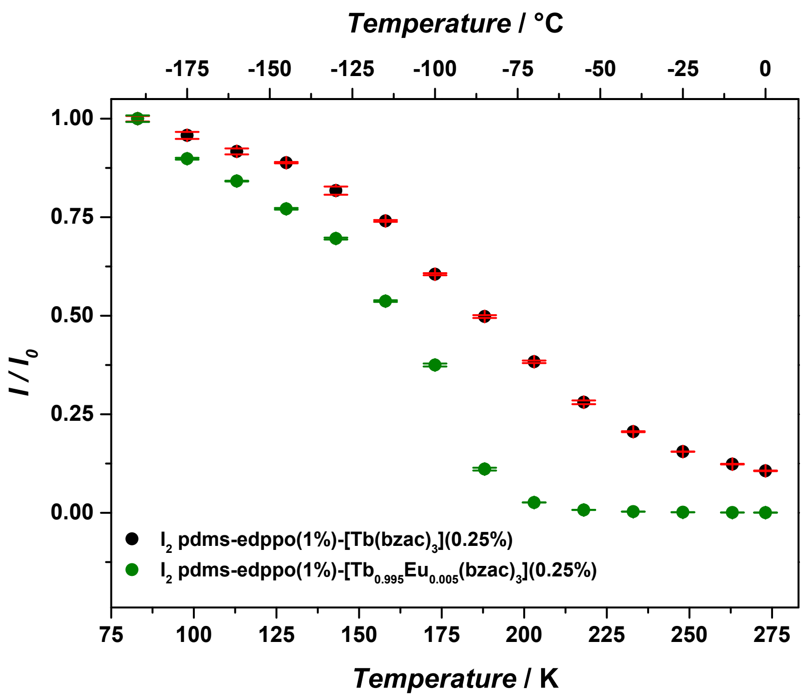

Figure S58: Temperature dependence of I_2 (integrated area of $^5D_4 \rightarrow {}^7F_5$ transition band) for pdms-eddpo(1%)-[$Tb(bzac)_3$](0.25%) and pdms-eddpo(1%)-[$Tb_{0.995}Eu_{0.005}(bzac)_3$](0.25%) membranes.

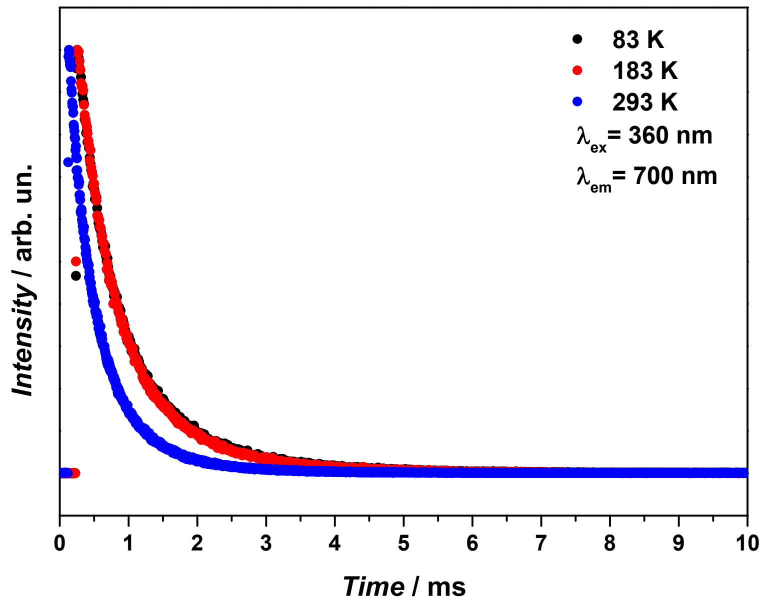

Figure S59: Decay curves of the $^5D_0$ emitter state for the pdms-eddpo(1%)-[$Tb_{0.9}Eu_{0.1}(bzac)_3$](0.25%) membrane.

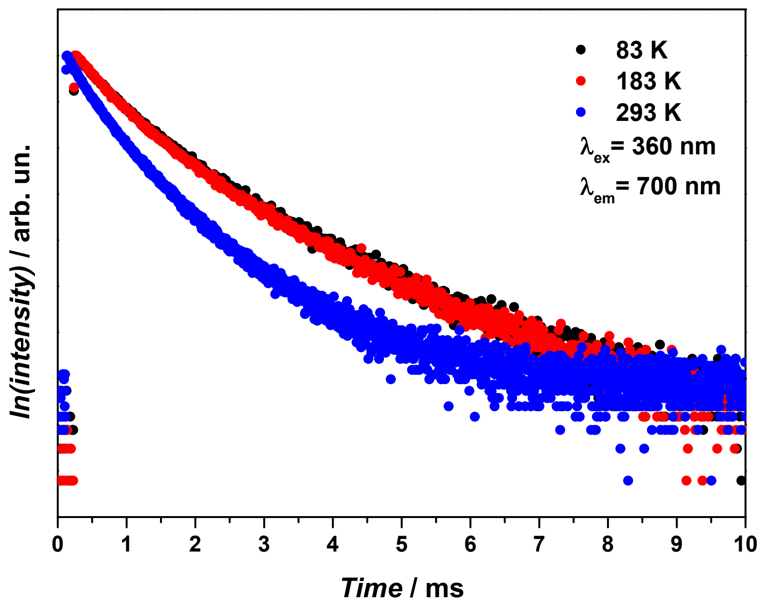

Figure S60: Linearization of the decay curves of the $^5D_0$ emitter state for the pdms-eddpo(1%)-[$Tb_{0.9}Eu_{0.1}(bzac)_3$](0.25%) membrane.

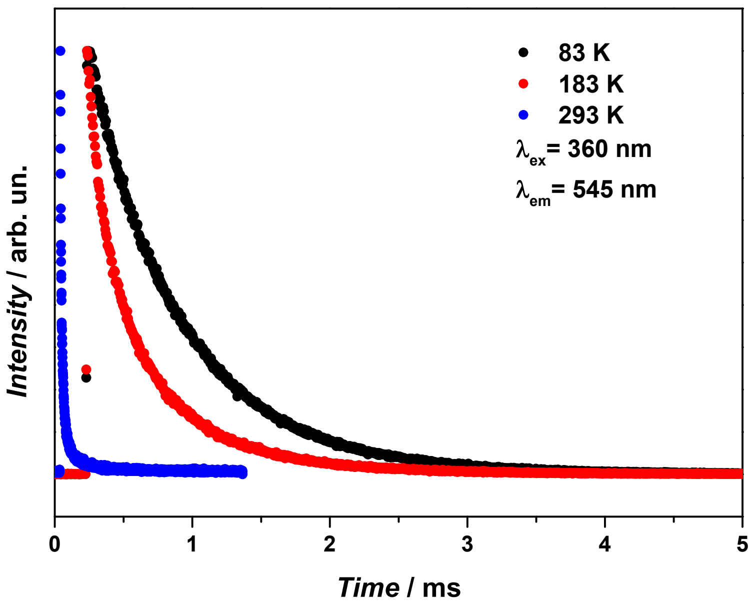

Figure S61: Decay curves of the $^5D_4$ emitter state for the pdms-eddpo(1%)-[$Tb_{0.9}Eu_{0.1}(bzac)_3$](0.25%) membrane.

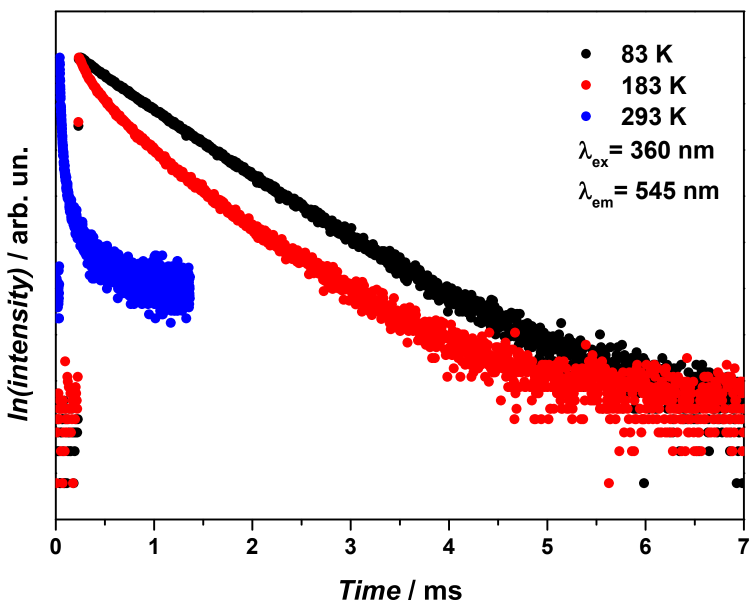

Figure S62: Linearization of the decay curves of the $^5D_4$ emitter state for the pdms-eddpo(1%)-[$Tb_{0.9}Eu_{0.1}(bzac)_3$](0.25%) membrane.

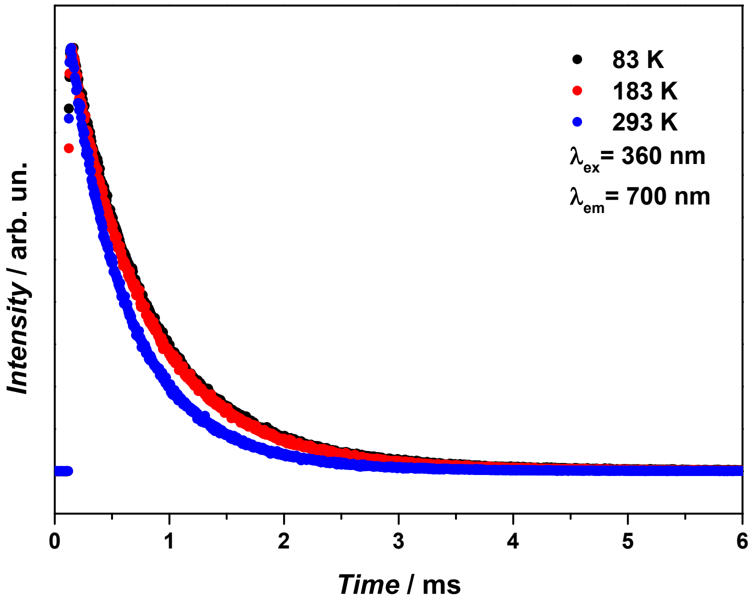

Figure S63: Decay curves of the $^5D_0$ emitter state for the pdms-eddpo(1%)-[$Gd_{0.9}Eu_{0.1}(bzac)_3$](0.25%) membrane.

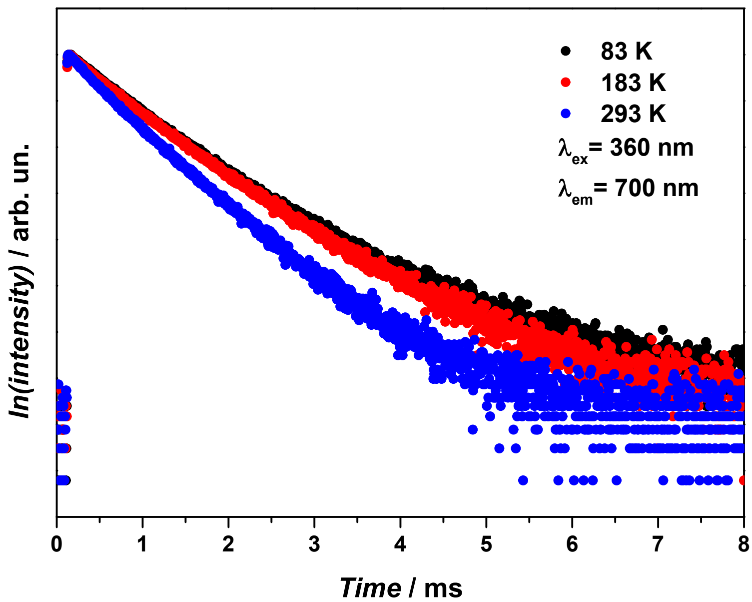

Figure S64: Linearization of the decay curves of the $^5D_0$ emitter state for the pdms-eddpo(1%)-[$Gd_{0.9}Eu_{0.1}(bzac)_3$](0.25%) membrane.

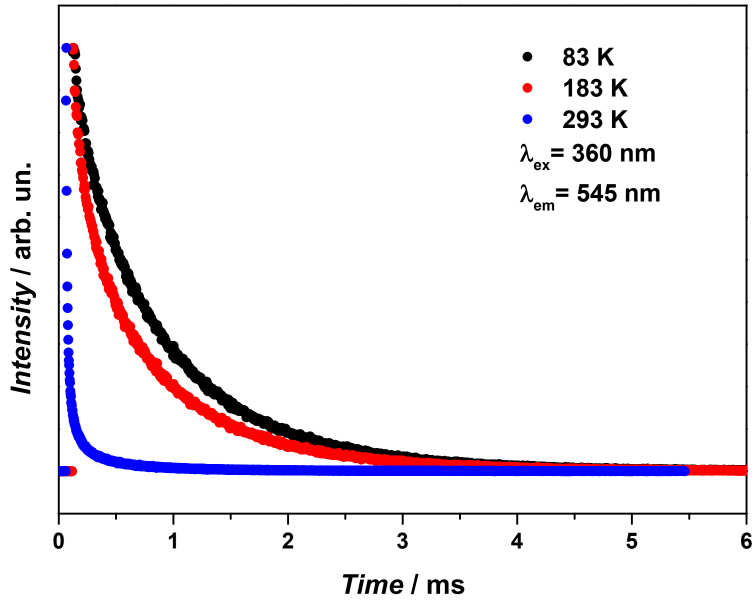

Figure S65: Decay curves of the $^5D_4$ emitter state for the pdms-eddpo(1%)-[$Tb_{0.9}Gd_{0.1}(bzac)_3$](0.25%) membrane.

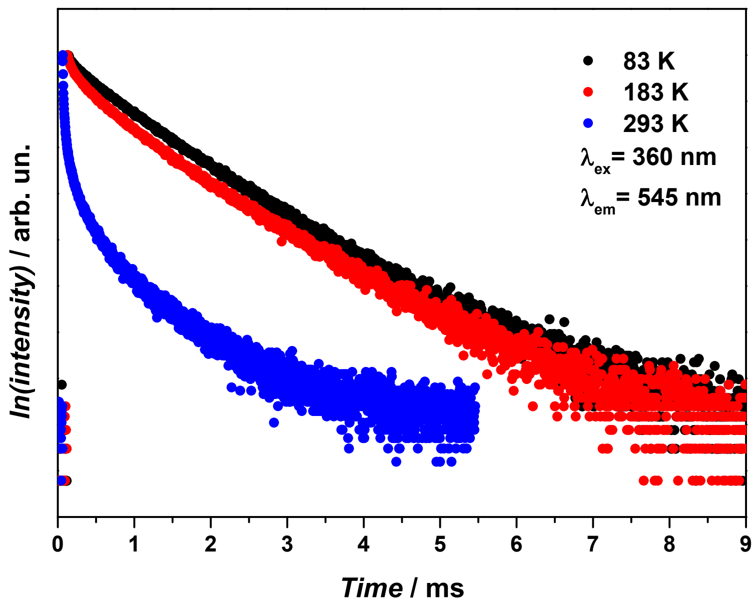

Figure S66: Linearization of the decay curves of the $^5D_4$ emitter state for the pdms-eddpo(1%)-[$Tb_{0.9}Gd_{0.1}(bzac)_3$](0.25%) membrane.

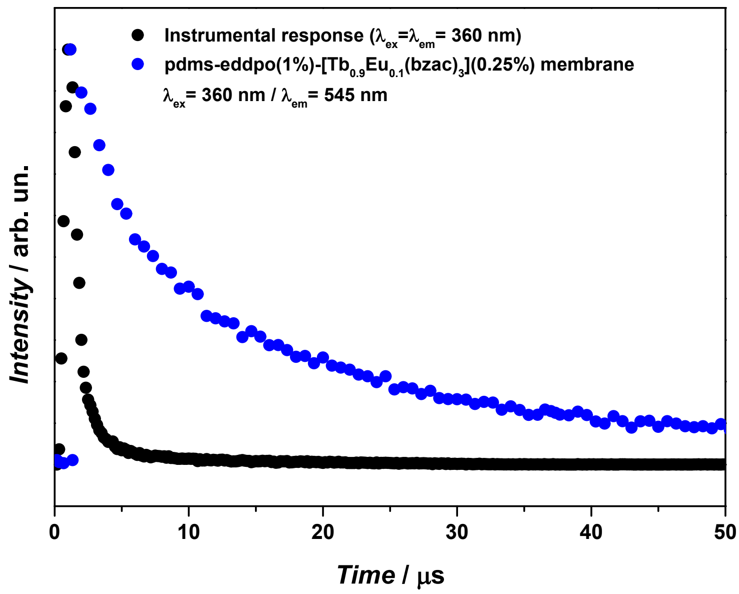

Figure S67: Instrumental response function (black point) with excitation and emission at 360 nm that results in an instrumental response lifetime of 736 ns and the comparison with part of the $^5D_4$ emission decay curves for the pdms-eddpo(1%)-[$Tb_{0.9}Eu_{0.1}(bzac)_3$](0.25%) membrane (the full decay curve is showed as the blue point of the Fig. S59).

Tables:

Table S1: Synthesized membranes in this work.

System	TVS / %*	edppo / %*	$[Ln(bzac)_3]$ / %**	Ln^{3+}
pdms	100	-	-	-
pdms-eddpo(1%)	99	1	-	-
pdms-eddpo(4%)	96	4	-	-
pdms-eddpo(4%)-$[La(bzac)_3]$(1%)	96	4	1	La^{3+}
pdms-eddpo(1%)-$[Gd(bzac)_3]$(0.25%)	99	1	0.25	Gd^{3+}
pdms-eddpo(1%)-$[Eu(bzac)_3]$(0.25%)	99	1	0.25	Eu^{3+}
pdms-eddpo(1%)-$[Tb(bzac)_3]$(0.25%)	99	1	0.25	Tb^{3+}
pdms-eddpo(1%)-$[Tb_{0.90}Eu_{0.10}(bzac)_3]$(0.25%)	99	1	0.25	0.9 Tb^{3+} / 0.1 Eu^{3+}
pdms-eddpo(1%)-$[Gd_{0.90}Eu_{0.10}(bzac)_3]$(0.25%)	99	1	0.25	0.9 Gd^{3+} / 0.1 Eu^{3+}
pdms-eddpo(1%)-$[Tb_{0.90}Gd_{0.10}(bzac)_3]$(0.25%)	99	1	0.25	0.9 Tb^{3+} / 0.1 Gd^{3+}
pdms-eddpo(1%)-$[Tb_{0.95}Eu_{0.05}(bzac)_3]$(0.25%)	99	1	0.25	0.95 Tb^{3+} / 0.05 Eu^{3+}
pdms-eddpo(1%)-$[Tb_{0.99}Eu_{0.01}(bzac)_3]$(0.25%)	99	1	0.25	0.99 Tb^{3+} / 0.01 Eu^{3+}
pdms-eddpo(1%)-$[Tb_{0.995}Eu_{0.005}(bzac)_3]$(0.25%)	99	1	0.25	0.995 Tb^{3+} / 0.005 Eu^{3+}

*percentual in relation of the initial molar quantity of Si-H groups of the pdms-H monomer.

**although no interaction occurs between the complexes and the Si-H groups of the pdms-H monomer, we expressed the percentage in relation to them.

Table S2: Elemental analysis and thermogravimetry data of the complexes.

Compound	C / %		H / %		Thermal stability / °C	Water / %		Final Residue / %		
	Calc.	Exp.	Calc.	Exp.		Calc.	TG	Calc.	TG	Oxide
$[La(bzac)_3(H_2O_2)]$	56.21	56.11	4.56	4.72	140	5.47	5.23	24.74	25.69	La_2O_3
$[Eu(bzac)_3(H_2O_2)]$	55.08	55.23	4.47	4.57	150	5.37	4.90	26.22	27.12	Eu_2O_3
$[Gd(bzac)_3(H_2O_2)]$	54.64	54.99	4.44	4.41	145	5.32	4.42	26.75	27.57	Gd_2O_3
$[Tb(bzac)_3(H_2O_2)]$	54.50	54.65	4.42	4.18	135	5.31	5.03	27.55	27.81	Tb_4O_7

Table S3: Emitter state ($^5D_0$ for Eu^{3+} in red/ $^5D_4$ for Tb^{3+} in green) lifetime values for some membranes.

System	$\tau_{(83K)}$ / µs		$\tau_{(183K)}$ / µs		$\tau_{(293K)}$ / µs	
	$^5D_0$	$^5D_4$	$^5D_0$	$^5D_4$	$^5D_0$	$^5D_4$
pdms-eddpo(1%)-[Eu(bzac)$_3$](0.25%)	692 ± 22 384 ± 27	-	660 ± 15 348 ± 21	-	531 ± 4 166 ± 5	-
pdms-eddpo(1%)-[Tb(bzac)$_3$](0.25%)	-	822 ± 18 362 ± 4	-	744 ± 4 227 ± 5	-	291 ± 19 37 ± 4
pdms-eddpo(1%)-[Tb$_{0.9}$Eu$_{0.1}$(bzac)$_3$](0.25%)	1195 ± 5 475 ± 3	708 ± 7 203 ± 3	1179 ± 14 468 ± 3	557 ± 6 138 ± 7	720 ± 31 298 ± 12	60 ± 4 8 ± 1
pdms-eddpo(1%)-[Gd$_{0.9}$Eu$_{0.1}$(bzac)$_3$](0.25%)	1041 ± 13 590 ± 17	-	901 ± 18 506 ± 8	-	625 ± 9 296 ± 16	-
pdms-eddpo(1%)-[Tb$_{0.9}$Gd$_{0.1}$(bzac)$_3$](0.25%)	-	941 ± 11 358 ± 14	-	882 ± 8 246 ± 10	-	463 ± 8 80 ± 9

Remarks on membrane synthesis:

The synthesis of the non-functionalized pdms membrane, was done (for control purpose) by the hydrosilylation reaction, where the Pt(0) catalyst promotes the reaction between the Si-H group of the pdms-H monomer and the vinyl group of the TVS cross-linker, resulting after the solvent evaporation in self-supported membrane (part 1 of Scheme 1 of the main text). Functionalization of the pdms monomer with the edppo ligand was achieved by the hydrosilylation reaction between a calculated molar quantity of the Si-H group of the pdms-H monomer and the allyl group of the adppo compound (part 2 of Scheme 1 of the main text). The remaining Si-H groups of the pdms-H monomer was reacted with the TVS cross-linker, resulting after the evaporation in self-supported membrane, named as pdms-edppo(n%), where n is the percentual of the Si-H groups functionalized with the edppo ligand. The highest functionalization content achieved was n= 4%, in concentrations above that, the membrane do not result on a self-supported system after the solvent evaporation.

For the attachment of the [Ln(bzac)$_3$(H$_2$O)$_2$] complexes, the pdms-H monomer was functionalized with the edppo ligand and before the reaction with the TVS cross-linker, the corresponding mass of the complex (calculated according to the percentage shown in Table 2 of the main text) has added to the solution. Here we take into account that each two edppo ligand coordinates with one $[Ln(bzac)_3(H_2O)_2]$ complex, through the substitution of the water molecules and added a molar ratio $[Ln(bzac)_3(H_2O)_2]$:adppo (1:4), an excess of 100% of the required adppo, to ensure that all complexes molecules reacts with two pdms-edppo monomer. The remaining Si-H groups of the pdms-H monomer was reacted with the TVS cross-linker, resulting after the evaporation in self-supported membrane, named as pdms-edppo(n%)-$[Ln(bzac)_3]$(m%), where n is the percentual of the Si-H groups functionalized with the edppo ligand and m is the percentual of the complex in relation to the initial Si-H groups (although the complex don't interact with the Si-H groups, we adopted this nomenclature to facilitate understanding and n = 4m). The example for the pdms-eddpo(1%)-$[Tb_{0.90}Eu_{0.10}(bzac)_3]$(0.25%) synthesis is presented below.

Synthetic procedure example:

Here we report the calculation involved on the synthetic procedure of the pdms-eddpo(1%)-$[Tb_{0.90}Eu_{0.10}(bzac)_3]$(0.25%) membrane. The procedure is described on the experimental section of the main text.

The molecular weight of the reagents and precursors is given below:

pdms-H = 580 g mol^{-1}

TVS = 136.27 g mol^{-1}

adppo = 242.25 g mol^{-1}

$[Eu(bzac)_3(H_2O)_2]$ = 671.55 g mol^{-1}

$[Tb(bzac)_3(H_2O)_2]$ = 678.51 g mol^{-1}

Functionalization of 1 grams of the pdms-H with 1% of the edppo ligand:

1 mole of pdms-H – 580 g

1.72×10^{-3} mole – 1 g

1 mole of pdms-H – 2 moles of Si-H

1.72×10^{-3} mole – 3.44×10^{-3} mole of Si-H

1 mole of adppo – 242.25 g

3.44×10^{-5} mole of adppo – 8.3 mg of adppo (used mass to the functionalization)

(1% of the Si-H bonds)

Attachment of the complexes on the functionalized matrix:

0.1 $[Eu(bzac)_3(H_2O)_2]$ - 0.9 $[Tb(bzac)_3(H_2O)_2]$ - 4 adppo

67.155 g mol^{-1}	610.66 g mol^{-1}	969 g mol^{-1}
0.575 mg	5.23 mg	8.3 mg

For the europium(III) complex, 100 µL of a 5.75 mg/mL solution in anhydrous toluene was used.

Addition of the cross-linker:

As 1 % of the Si-H bonds were functionalized with the edppo ligand, the remaining 99% of the bonds are reacted with the TVS cross-linker:

1 mole of TVS – 136.27 g

3.41×10^{-3} mole of TVS – 464.7 mg of TVS

(99% of the Si-H bonds)

As each TVS molecule can react with 4 Si-H bonds, the used mass of the cross-linker is approximately 116.2 mg.